AD-A044 166 WENTWORTH INST BOSTON MASS F/G 17/5
MODEL SENSOR FOR PROJECT ZIP.(U)
MAR 77 J M OTIS F19628-76-C-0211
UNCLASSIFIED SCIENTIFIC-1 AFGL-TR-77-0088 NL

1 OF 2
ADA044166

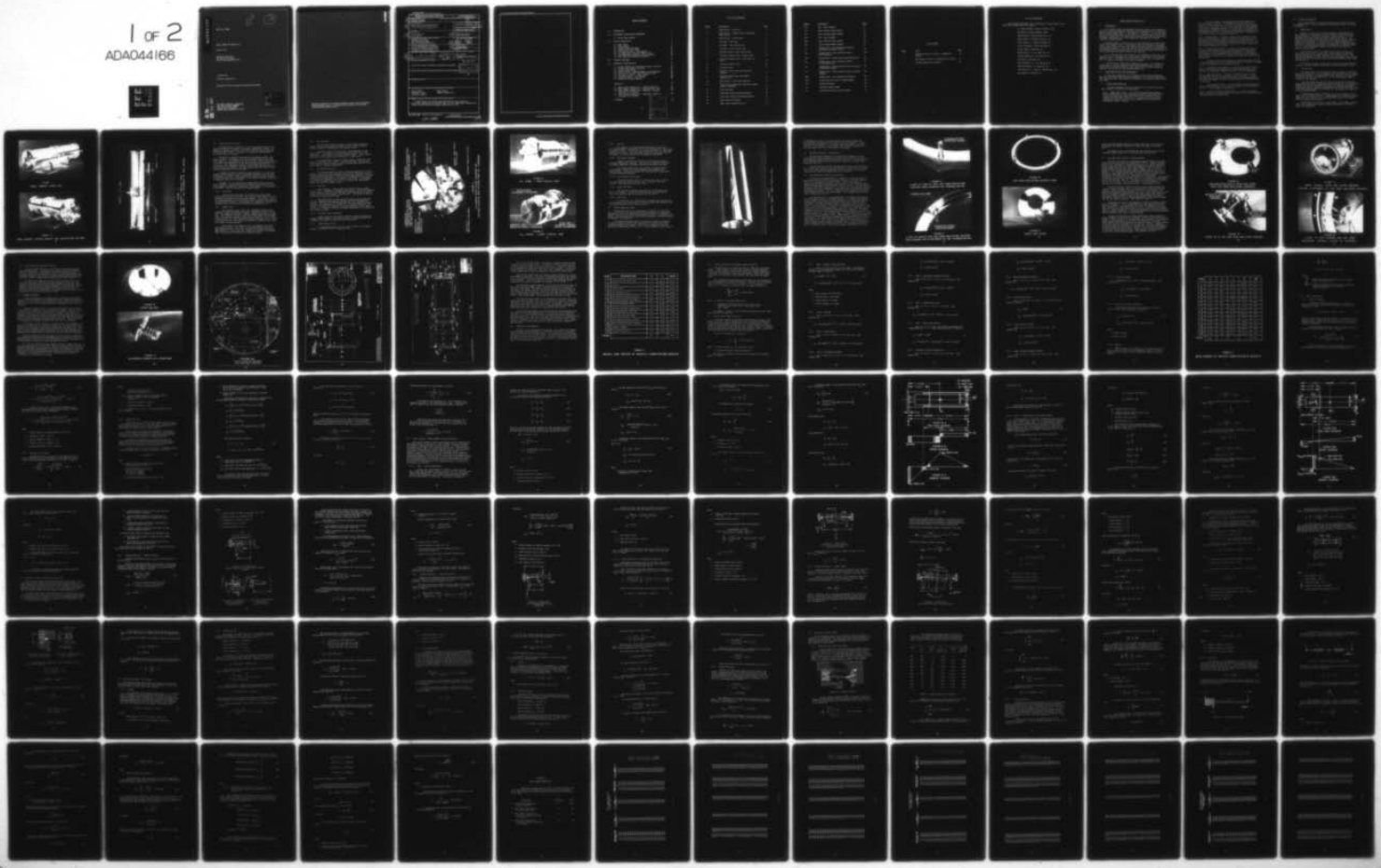

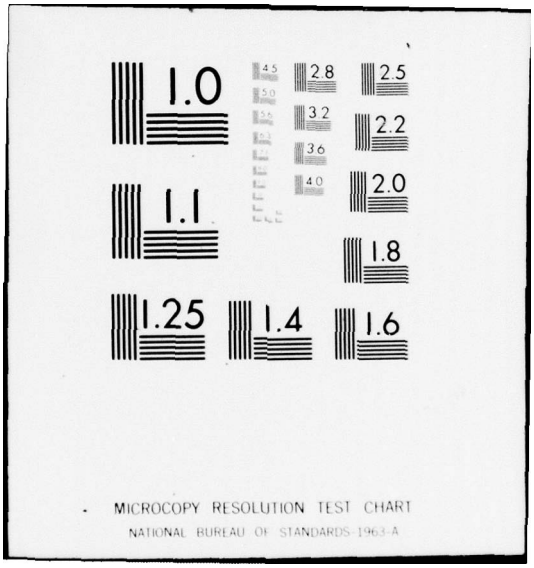
1.0
1.1
1.25
1.4
1.6
1.8
2.0
2.2
2.5
2.8
3.2
3.6
4.0
4.5
5.0
MICROCOPY RESOLUTION TEST CHART
NATIONAL BUREAU OF STANDARDS-1963-A

AFGL-TR-77-0088

MODEL SENSOR FOR PROJECT ZIP

John M. Otis

Wentworth Institute
550 Huntington Avenue
Boston, Massachusetts 02115

31 March 1977

Scientific Report No. 1

Approved for public release; distribution unlimited.

AIR FORCE GEOPHYSICS LABORATORY
AIR FORCE SYSTEMS COMMAND
UNITED STATES AIR FORCE
HANSCOM AFB, MASSACHUSETTS 01731

Unclassified

SECURITY CLASSIFICATION OF THIS PAGE (When Data Entered)

REPORT DOCUMENTATION PAGE	READ INSTRUCTIONS BEFORE COMPLETING FORM
1. REPORT NUMBER: AFGL-TR-77-0088	2. GOVT ACCESSION NO. — 3. RECIPIENT'S CATALOG NUMBER
4. TITLE (and Subtitle): Model Sensor for Project ZIP.	5. TYPE OF REPORT & PERIOD COVERED: Scientific - Interim rept.
	6. PERFORMING ORG. REPORT NUMBER: Scientific Report No. 1
7. AUTHOR(s): John M. Otis	8. CONTRACT OR GRANT NUMBER(s): F19628-76-C-0211 new
9. PERFORMING ORGANIZATION NAME AND ADDRESS: Wentworth Institute, 550 Huntington Avenue, Boston, Massachusetts 02115	10. PROGRAM ELEMENT, PROJECT, TASK AREA & WORK UNIT NUMBERS: 62101F 76700607 17 06
11. CONTROLLING OFFICE NAME AND ADDRESS: Air Force Geophysics Laboratory, Hanscom AFB, Massachusetts 01731, Monitor/C.Nealon Stark/LCR	12. REPORT DATE: 31 March 1977 — 13. NUMBER OF PAGES: 100
14. MONITORING AGENCY NAME & ADDRESS (if different from Controlling Office): Scientific-1 12 99p.	15. SECURITY CLASS. (of this report): Unclassified — 15a. DECLASSIFICATION/DOWNGRADING SCHEDULE

16. DISTRIBUTION STATEMENT (of this Report)

Approved for public release; distribution unlimited

DDC RECEIVED SEP 15 1977 B

17. DISTRIBUTION STATEMENT (of the abstract entered in Block 20, if different from Report)

18. SUPPLEMENTARY NOTES

19. KEY WORDS (Continue on reverse side if necessary and identify by block number)

Vacuum Vessel
Radiation Shield
Insulating Support
Model Sensor
Thermal Conductivity

20. ABSTRACT (Continue on reverse side if necessary and identify by block number)

A Model Sensor was designed and fabricated for the purpose of developing component parts and techniques for the rocket-born, cryogenically cooled infrared sensing instrument, referred to as ZIP.

DD FORM 1 JAN 73 1473 EDITION OF 1 NOV 65 IS OBSOLETE

Unclassified

SECURITY CLASSIFICATION OF THIS PAGE (When Data Entered)

373800

TABLE OF CONTENTS

LIST OF ILLUSTRATIONS

LIST OF TABLES

LIST OF CONTRIBUTORS

The following individuals have contributed in various phases to the Model Sensor described in this report:

Dr. Thomas Murdock, Project Scientist, AFGL

Roy Walters, Project Engineer, AFGL

Howard Benassi, Machine Shop Supvr., WI

Robert Charron, Electronics Supvr., WI

Paul Hartnett, Sr. Design Draftsman, WI

Daniel Stremeckus, Design Draftsman, WI

Francis Marino, Draftsman, WI

Rudolph Cabral, Sr. Exp. Machinist, WI

Alfonso Gambale, Sr. Exp. Machinist, WI

John Dennis, Machinist, WI

George Petersen, Sr. Exp. Machinist, WI

Walter Ortendahl, Exp. Machinist, WI

John Kavolius Jr., Faculty - Welding Dept., WI

Amy Gaiennie, Secretary, WI

MODEL SENSOR FOR PROJECT ZIP

1.0 INTRODUCTION

This report presents the mechanical design and results of an engineering analysis performed by Wentworth Institute on the component parts for the cryogenically cooled Model Sensor -- the subject of this report. It also concludes the preliminary design phase and will serve as a reference source in the final design and construction of a rocket-borne cryogenically cooled infrared sensing instrument, designated by Air Force Geophysics Laboratory as ZIP Sensor (Zodiacal Infrared Project).

The Model Sensor is comprised of a flight-qualified liquid helium dewar assembly and component parts. The component parts are defined as the vacuum vessel, cover plates, telescope mass mock-up, radiation shield, and low temperature supporting devices. It is also the aim here to define the configuration and interface control specifications for the liquid helium dewar (see figure 19) and the telescope base mounting flange (see figure 20).

It is the intent that the assembly of the component parts be used as an apparatus for the acceptance tests of the dewar's performance, which include a vibration test -- to evaluate its structural integrity; and a low temperature test -- to measure the dewar's hold time performance.

The Model Sensor, fabricated by Wentworth Institute is a prelude to a primary goal -- the fabrication and assembly of component parts for two (2) rocket-borne ZIP Sensor assemblies, each scheduled for separate launchings. Woomera, South Australia is the selected launch site.

2.0 PRELIMINARY DESIGN PHASE REQUIREMENTS

In the early conception of this project, meetings were scheduled at AFGL for the purpose of establishing requirements. The following requirements were transcribed from those meetings and represent the essential requisites for this phase.

2.1 Design Phase Objectives

This part represents the goals toward which the engineering efforts were directed in satisfying the requirements.

2.1.1 Model Sensor Layout -- To provide a proposed design layout drawing delineating the major supporting components of the Model Sensor giving consideration to simplicity regarding the components' access, assembly and disassembly feasibility. To determine its total weight, longitudinal center of gravity and mass moment of inertia about the longitudinal center of gravity.

The specifications that governed the design boundaries for this phase were as follows -- The body diameter was not to exceed 11 inches. The total length was to include an estimated 9 liter capacity liquid helium (LHe) dewar and 25 inch long telescope structure mounted to the dewar's coldworking surface. Its weight was not to exceed 100 pounds and all mechanical joints had to be designed to withstand a loading condition of 100 "g's" at both ambient and cryogenic temperatures, in both the lateral and longitudinal directions.

2.1.2 Vacuum Vessel -- To design a vacuum vessel capable of safely holding and maintaining a vacuum of 10^{-5} torr for seven hours with a leak rate not to exceed one order of magnitude for that duration. To provide structural reinforcement and mounting attachments for the outside of the vessel, at the system's longitudinal center of gravity, for the purpose of gimbaling the sensor.

2.1.3 Telescope Mass Mock-up -- To design a telescope mass mock-up structure, base mounted at one end and supported at the other with flexibility in it to accommodate thermal contraction. To determine and document the specifications of the telescope structure's mounting base in regards to feature size, method of attachment and surface finish requirements.

The design control specifications for this phase were as follows -- The body diameter was not to exceed eight inches, its length, 25 inches; and the total weight was not to exceed 20 pounds.

2.1.4 Liquid Helium (LHe) Dewar -- To determine the dewar's configuration and prepare the documentation for the specifications of the feature size, attachment methods and dimension control requirements.

2.1.5 Radiation Shield -- To design a radiation shield to shield the telescope structure from the outer vessel's inner wall. It was specified that the shield be base mounted at one end and supported at the other with adequate flexibility to accommmodate thermal contraction in the metal.

Design Specifications -- For the purpose of heat transfer calculations, the temperature of the shield was assumed to operate between 50^{o} to 77^{o} K at a steady state temperature.

2.1.6 Low-Temp Insulating Support Devices -- To design insulating support devices as required for both front ends of the telescope structure and radiation shield, respectively.

3.0 PHYSICAL DESCRIPTION

This section presents a general explanation of the Model Sensor and its component parts. They are pictorially illustrated in figures 1 through 17 inclusive.

3.1 Model Sensor

Figures 1, 2 and 3 illustrate the assembly of the Model Sensor. Its cylindrical configuration is simply an aluminum vacuum vessel with flat end closures. The front end closure, shown in figure 1, is a demountable thick plate sealed and tightly secured to the vessel. The flight sensor version of the front cover will, however, have an objective function in the assembly. The front end of the sensor requires a removable cover, which seals an aperture through which the telescope views. The cover is retained to the vessel by one atmosphere of pressure acting on it. A lab jack mechanism attached to the face of the cover will remove it during flight.

The rear end closure of the Model Sensor, shown in figure 2, is also a thick plate and is a part of the liquid helium (LHe) container. Together they make up the dewar assembly, (see figures 5 and 6). The rear end closure plate is the primary load carrying member in this system. The radiation shield, telescope, and liquid helium container are all cantilevered from it.

The aluminum surface of the model is highly polished and thoroughly cleaned to minimize radiation heat emission through the vessel's walls.

3.2 Vacuum Vessel

The vacuum vessel with end closures shown in figure 3 is the basic housing for the system. It is assembled in two cylindrical halves, sealed and bolted together. The double flanged joint located just to the right of the test lug shows this connection. An "O"-ring face seal gland is provided in the interface.

The thick flanges on each end of the vessel provide the rigidity required for securing and maintaining a tight vacuum seal. A parallel ring spaced to the left of the double flanged joint in figure 3 gives added reinforcement for two, opposite cross members bridging the two rings. The rings serve another purpose in the design, as they enhance the stability of the cylindrical shell.

A wedge-shaped socket is machined into the cross members, at the gimbal axis, for sensor mounting. A wedge-shaped plug (referred to as the gimbal test lug in figure 3) is shown engaged and seated in the socket. Both are securely bolted together.

The function of the vessel in the assembly is to maintain a vacuum tight system around the telescope and dewar sub-assembly to insulate against gas conduction.

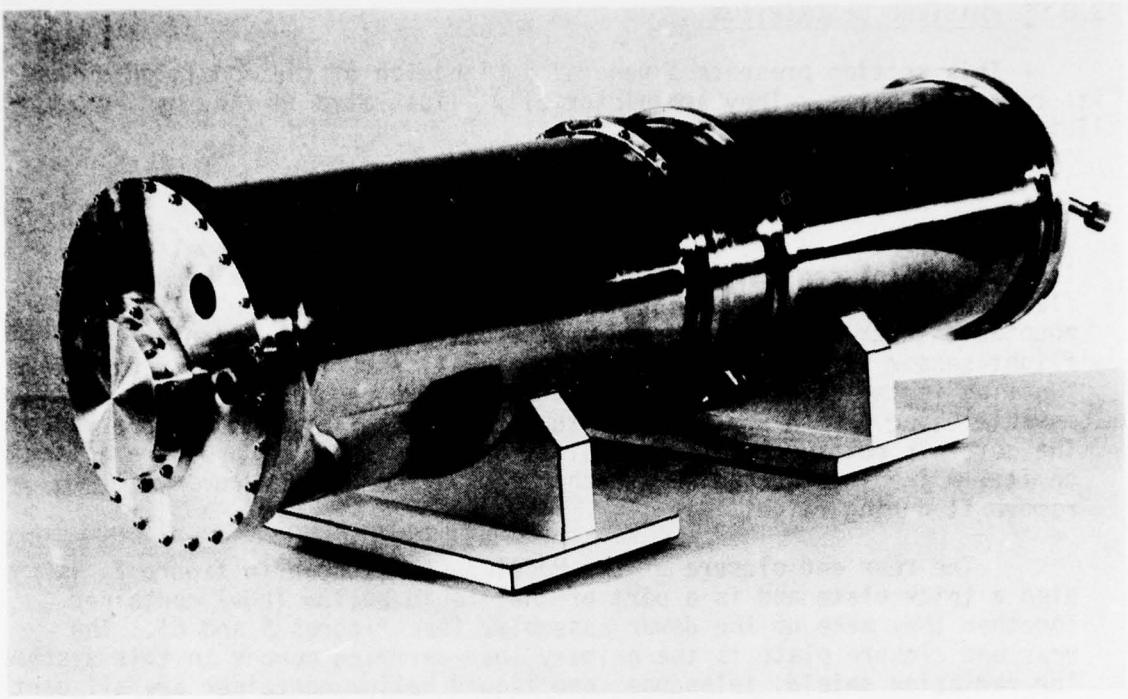

FIGURE 1

MODEL SENSOR – FRONT END

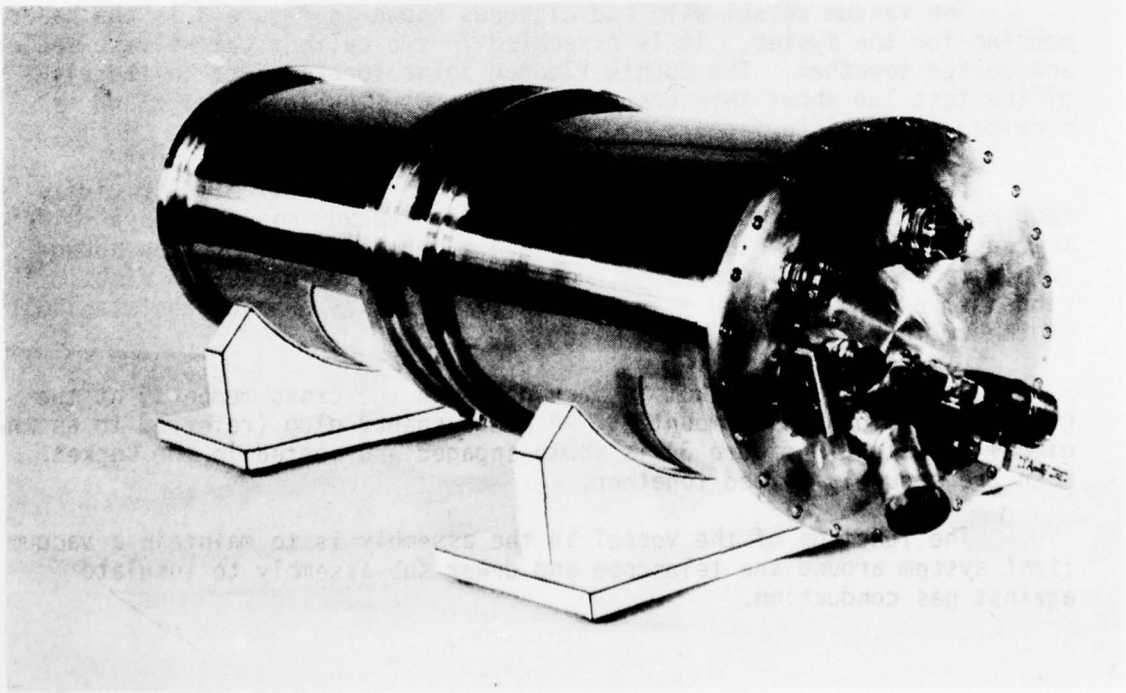

FIGURE 2

MODEL SENSOR – CRYOGEN SERVICE AND VACUUM PUMP OUT END

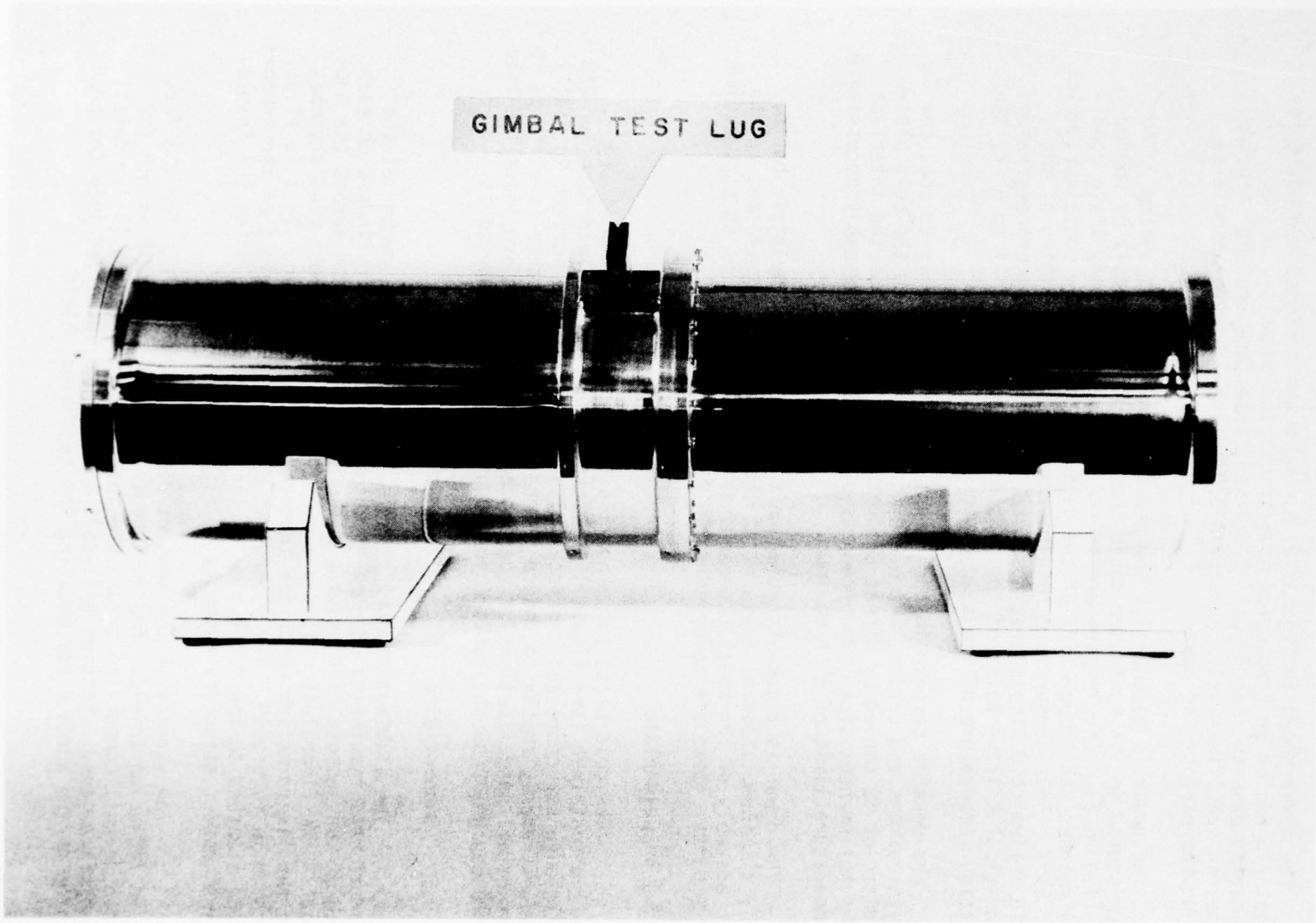

FIGURE 3

MODEL SENSOR – PROFILE VIEW
SHOWING THE GIMBAL TEST LUG ATTACHED TO THE VESSEL

3.3 Liquid Helium (LHe) Dewar

The dewar shown in figures 4, 5, and 6 was designed and built for Project Zip Sensor by Cryogenics Associates, Indianapolis, Indiana. An engineering drawing (see figure 19) titled "Interface Drawing" provided the design specifications. Paragraph 3.3 defines the sub-assemblies delivered as part of the dewar.

The dewar is essentially the heart of the sensor's system. The helium stored in its container cools the cold plate directly by conduction (figure 6). The temperature of the cold plate (steady state condition) reaches the temperature of the helium stored in the container, which is at 6^{0} K. This temperature results from the pressurization of the liquid helium to 3 atmosphere, absolute, during which the process raises the critical boiling point of the liquid helium from 4.2^{0} K to 6^{0} K, the operating temperature of the cold plate.

The dewar's purpose in the flight sensor assembly is to cool the detector arrays and optics, which are mounted directly on the cold plate. The detector is cooled by direct conduction of heat across the interface to the helium heat sink. Requirements of the detector assembly necessitate a temperature limit of 6^{0} K maximum.

The dewar is a sub-assembled unit constructed of multiple parts, mostly aluminum. Several features of those parts are significant to the basic assembly of the model's components. The following is an explanation of the parts. Some are referred to in figures 4 and 6.

3.3.1 Cold Plate

The cold plate (aluminum) is the front end of the liquid helium container (see figure 19). This surface is the interface for the telescope structure and the focal plane detector. The surface is flat and extrememly smooth to reduce thermal contact resistance (see figure 19 for detail specifications). Locking heli-coil inserts are installed into threaded holes on the surface for mounting the telescope to it.

3.3.2 Support Ring

The aluminum support ring is the intermediate member of the container's insulating support structure. Fiberglass cylinders on each end of the support ring provide a thermal impedance path across the support. The fiberglass cylinder to the left of the support ring attaches to the liquid helium container through an aluminum ring. This is illustrated in figure 19. The fiberglass cylinder to the right of the support ring attaches to the front side of the end cover, completing the insulating support structure assembly.

The surface of the support ring is the interface for the forward radiation shield. The surface is flat and extremely smooth for good thermal conduction across the interface (see figure 19 for detail specifications). Locking heli-coil inserts are installed into threaded holes on the surface for mounting the radiation shield.

3.3.3 Rear End Cover

The end cover (aluminum) attaches to the thermal insulating support structure and container assembly and thus, forms the dewar's external cylindrical configuration (see figures 5 and 6).

The inner surface of the end cover is the interface for the vacuum vessel. The surface is flat and extremely smooth for a tight vacuum seal. (See figure 19 for detail specifications). Clear, counterbored holes on the surface are for mounting it to the vessel.

A low temperature insulating support device is attached to the cover at its center on the inside. This device supports the free end of the container against lateral forces and enables the container to contract freely at cryogenic temperatures.

3.3.4 Aft Radiation Shield

An aluminum cylindrical shield, interposed between the insulating support structure and inner container, serves as an interceptor to some of the radiation that would otherwise be transmitted directly to the inner container from the outer wall. The shield is hardmounted to the support ring between the fiberglass tube extending to the right. A low temperature insulating support device, as in 3.3.3 supports the free end and enables the shield to contract freely.

3.3.5 Vent Tube

Copper tubing is coiled around the radiation shield, forming several coils. The tubing is attached to the shield. One end is connected to the cryogenic container while the other passes through the end cover, connecting to the valve plumbing (see figure 4). This serves as the vent line for the system's boil-off gas.

The sensible heat of the vaporized liquid is used to intercept the heat conducted to the container through the system's mechanical supports. The vapor gas flows through the vent tube, around the shield and out to the surroundings, carrying with it the heat absorbed in the system. This process is referred to as vapor shielding, and its design principle is utilized to maintain a constant temperature at the forward and aft radiation shields.

3.3.6 MLI (Multi-layer insulation)

Several layers of thin highly reflecting radiation shields are wrapped around the dewar's cylindrical surface to reduce radiative heat transport (see figures 5 and 6) from the vacuum vessel.

3.3.7 Vacuum Pump-out Valve

Air between the outer vessel and inner container is evacuated through a Cryolab #SUI-88-1W1 evacuation valve.

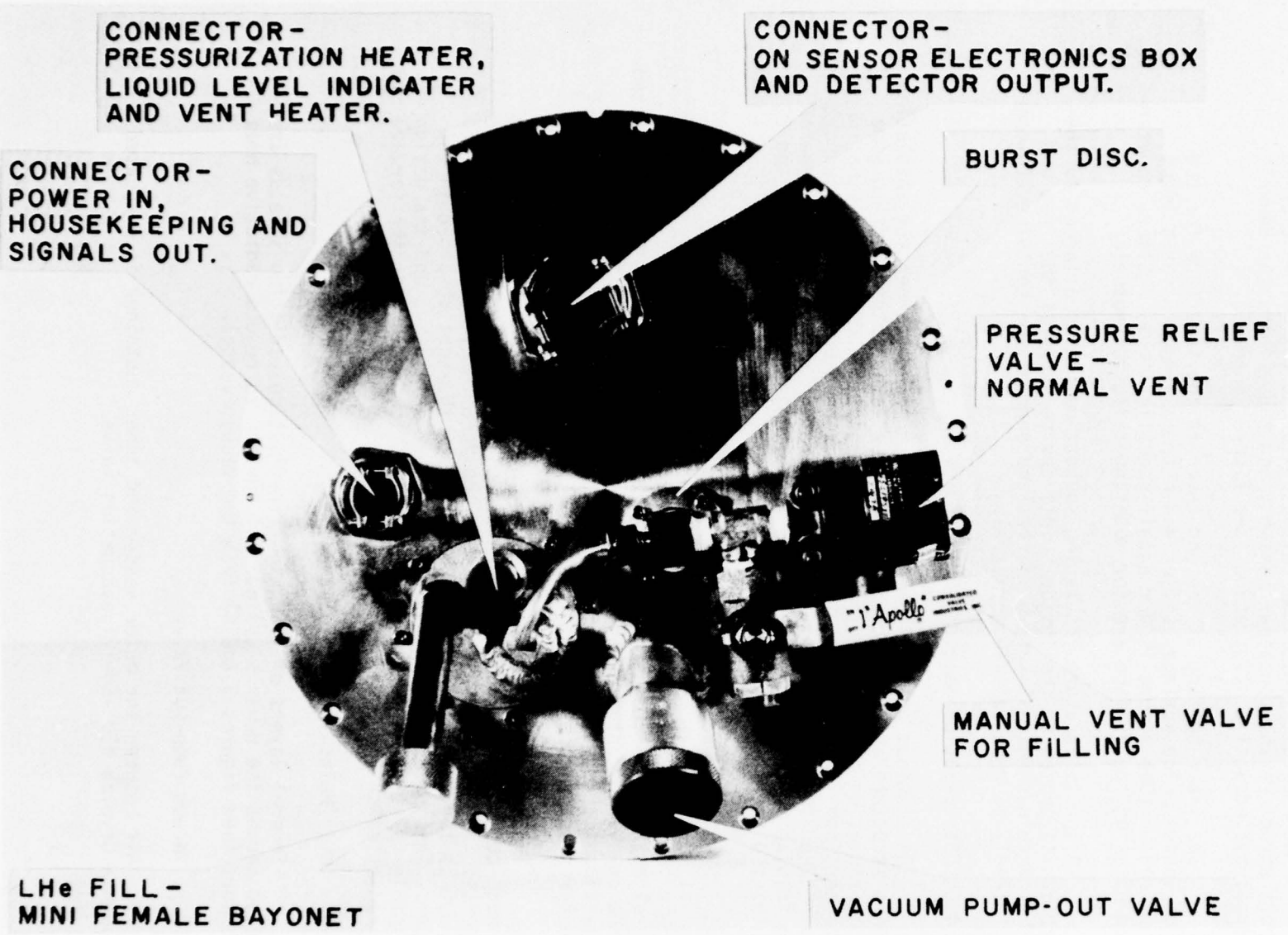

FIGURE 4

LHe DEWAR-REAR PLATE SHOWING THE
CRYOGEN SERVICE AND VACUUM PUMP OUT HARDWARE.

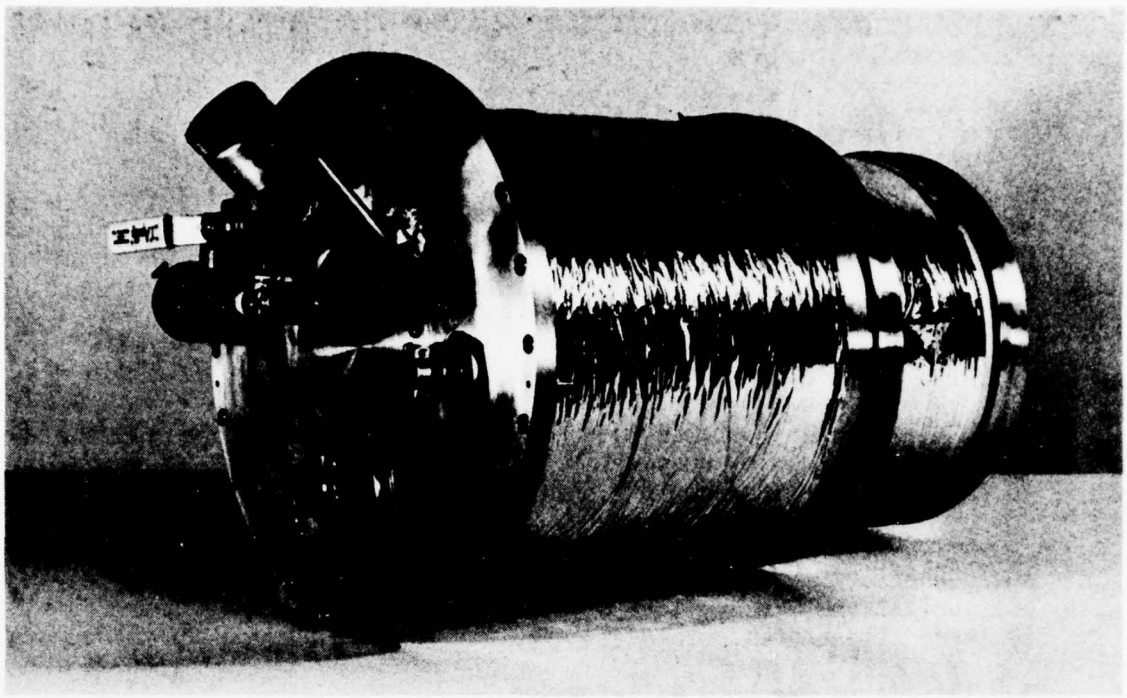

FIGURE 5

LH_e DEWAR – REAR PROFILE VIEW

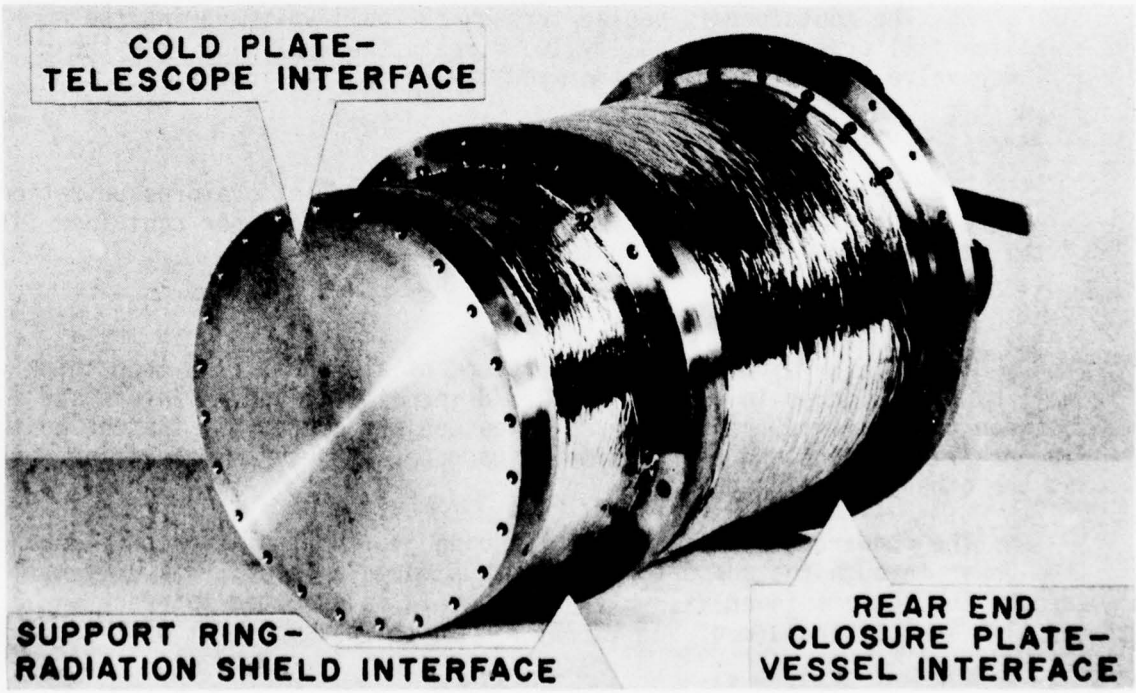

FIGURE 6

LH_e DEWAR – FRONT PROFILE VIEW

3.3.8 LHe Fill

The container is filled through the Cryogenic Associates' mini-female bayonet. The bayonet is a vacuum insulated unit, constructed of stainless steel. The unit consists of an outer jacket and inner tube, concentrically spaced. The inner tube extends into the vacuum space of the dewar, is coiled, inserted into the container and sealed.

3.3.9 Vent Heater Connector

A heater installed near the exit of the vent line receives its power through this connector. The vent gas is heated at the exit to ambient temperature to prevent frosting on the exterior surface.

The pressurization heater also receives its power through the connector. Heater strips are attached to the container for pressurization. Through this device, the liquid helium is pressurized to three atmospheres absolute.

3.3.10 Tavco Pressure Relief Valve

The pressure relief valve is a safety device that is open to the inner container through the vent line. The valve limits the pressure in the container to 45 PSI (3 atm).

3.3.11 Manual Ball Valve

The container is vented through the ball valve during the helium fill process. The ball valve directs the vent flow from the Tavco valve (normal vent) to the manual vent for filling.

3.3.12 Burst Disc

The Burst Disc is a safety device to prevent overpressurization of the vacuum vessel in the event of a leak from the inner container into the vacuum space and set to rupture at 60 PSI.

3.4 Forward Radiation Shield

The shield (figure 7) is constructed of aluminum, 1/16 inch thick wall by 9 1/2 inches in diameter by 30 5/8 inches long and is interposed between the walls of the vessel and telescope structure. It fastens to the support ring at one end and is simply supported through an insulating device at the other (see figure 20).

The forward radiation shield is joined to the radiation shield of the dewar through the support ring and thus forms a shield, gas driven, around the systems inner assembly. The shield is expected to reach an equilibrium temperature of 50^{o} to 77^{o} K. In the assembly, it will serve as

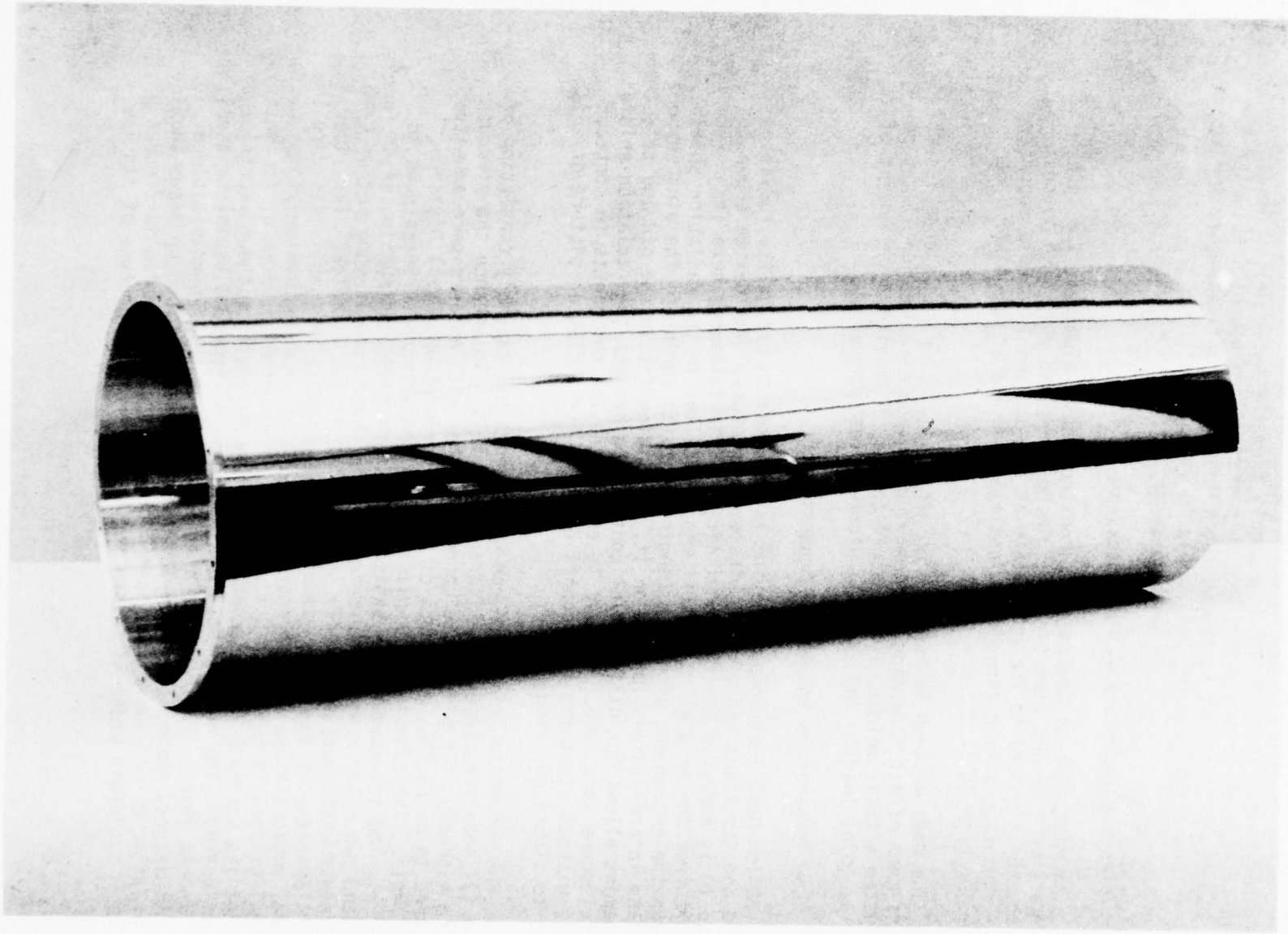

FIGURE 7

RADIATION SHIELD – REAR PROFILE VIEW

an interceptor to some of the radiation flux that would otherwise be transmitted to the system's inner assembly from the outer wall. Since its equilibrium temperature is lower than that of the vessel's hot wall (300^{o} K), it will radiate to the system's inner cold wall assembly (6^{o} K) with less power than the hot wall would in its absence.

3.5 Telescope Structure -- Mass Mock-up

The mass mock-up component is constructed of aluminum, 1/4 inch thick wall by 8 inches diameter by 25 inches long and weighs 20 pounds. The structure fastens to the cold plate at one end and is simply supported by the radiation shield through an insulating device at the other (see figure 20, view "A").

The mass mock-up basically simulates the 20 pound telescope assembly for its mass effect regarding the contribution and distribution it has on the system's total weight, longitudinal center of gravity, mass moment of inertia, joint loading and thermal interface resistance.

3.6 Low Temperature Insulating Support Ring

A low heat leak support device is required to bridge the radiation shield and the front end of the telescope structure. The device shown in figure 10 is employed for that application. The telescope gets its support from the insulating support ring installed in the radiation shield, through the engagement of pins extending from its surface. The pins support only the lateral forces imposed on it. A sliding fit in the pin and telescope engagement allows for differential contraction between the radiation shield and telescope structure. This is to enable the two components to contract freely without stressing the support device. For a clearer picture of this, refer to figure 20, view "A".

The supporting ring is a non-homogeneous sub-assembly consisting of three (3) separate pieces of different materials. To enhance the strength of the assembly, the pieces are bonded together with an aerospace adhesive referred to as EA 934, a product of Dexter Corporation, Hysol Division, California. The adhesive is applicable for temperature services down to -423^{o} F. The sub-assembly is basically a sandwiched construction of an inner ring and two outer ring reinforcements. The inner ring is made out of G-10 fiberglass with four (4) equally spaced lobes on its diameter. The inner fiberglass ring is the major element in the assembly because it has very low thermal conductivity. This property makes it an excellent material to use for thermal bridges in cryogenic systems. Other important aspects of the material is that its strength increases as temperature decreases without sacrifice of impact energy. The outer pieces are both made of type 304 stainless steel, .018 inches thick. Their function is to reinforce the fiberglass piece against induced thermal stresses and imposed forces. Close up views showing the reinforcment of the fiberglass inner ring are illustrated in figures 8 and 9. Stainless steel is chosen for the outer rings because of its low

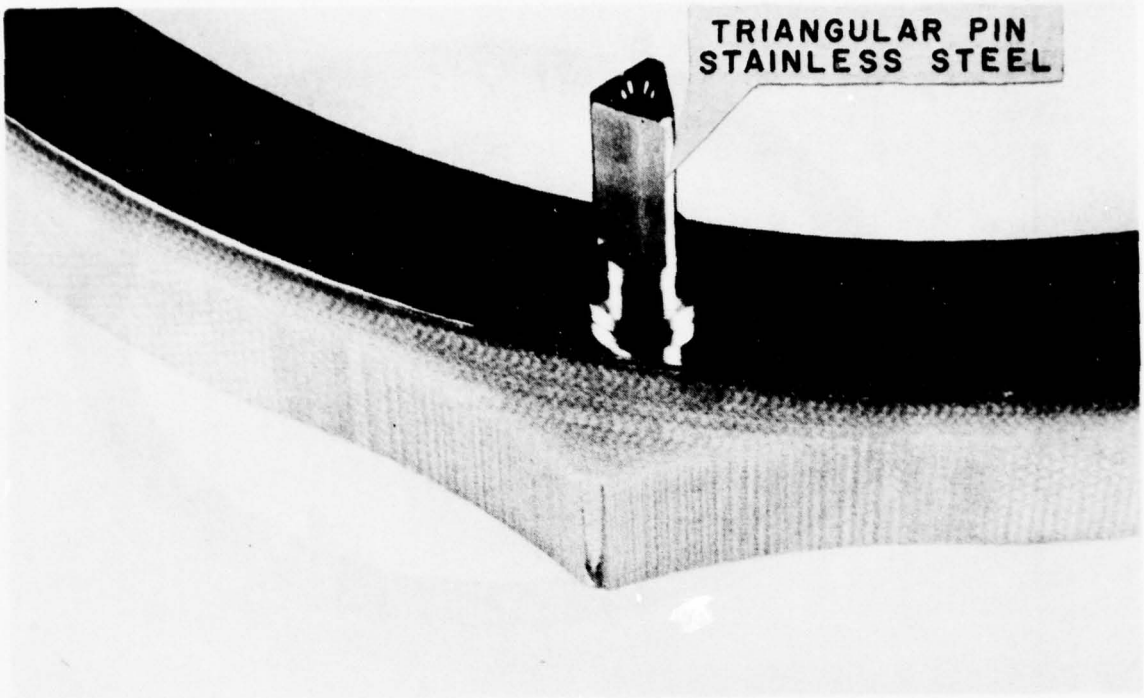

FIGURE 8
CLOSE UP VIEW OF THE LOW TEMP. INSULATING SUPPORT RING SHOWING THE TRIANGULAR PIN.

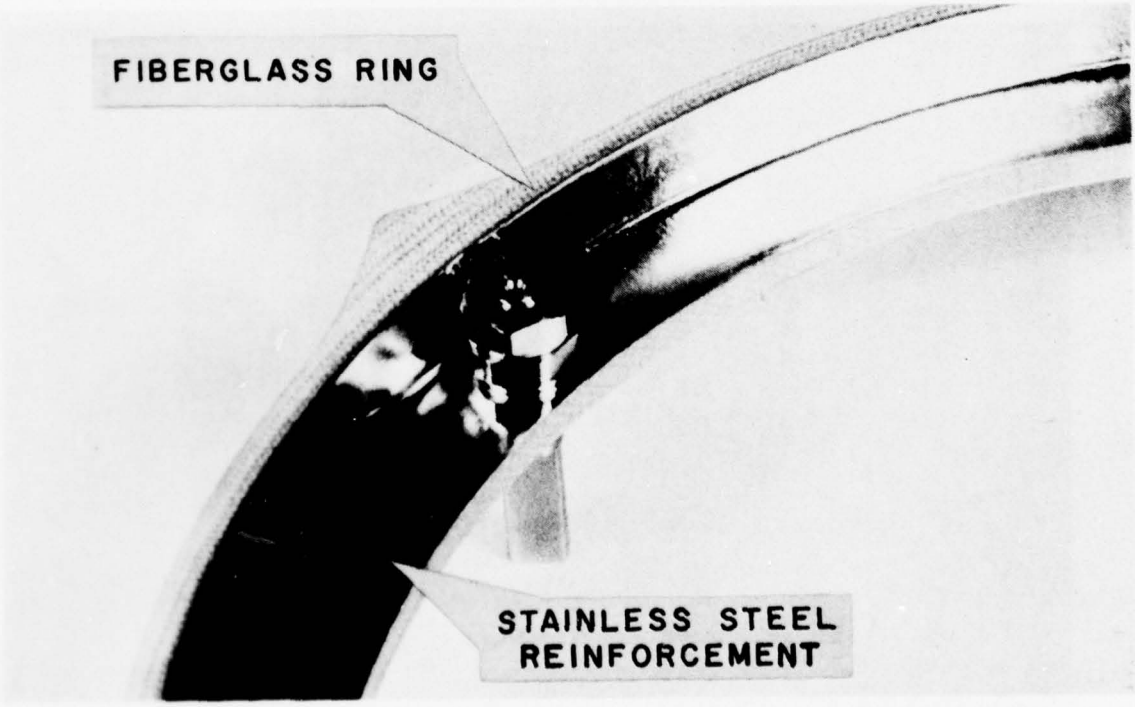

FIGURE 9
CLOSE UP VIEW OF THE LOW TEMP. INSULATING SUPPORT RING SHOWING THE ATTACHMENT OF THE TRIANGULAR PIN.

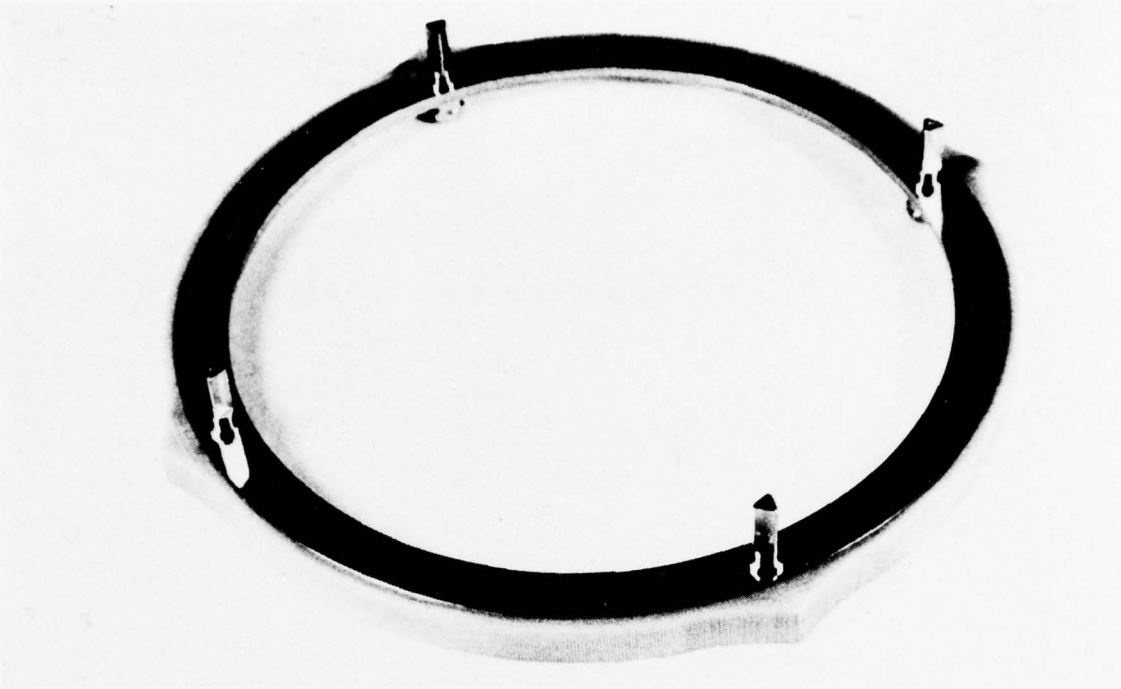

FIGURE 10
LOW TEMP. INSULATING SUPPORT RING

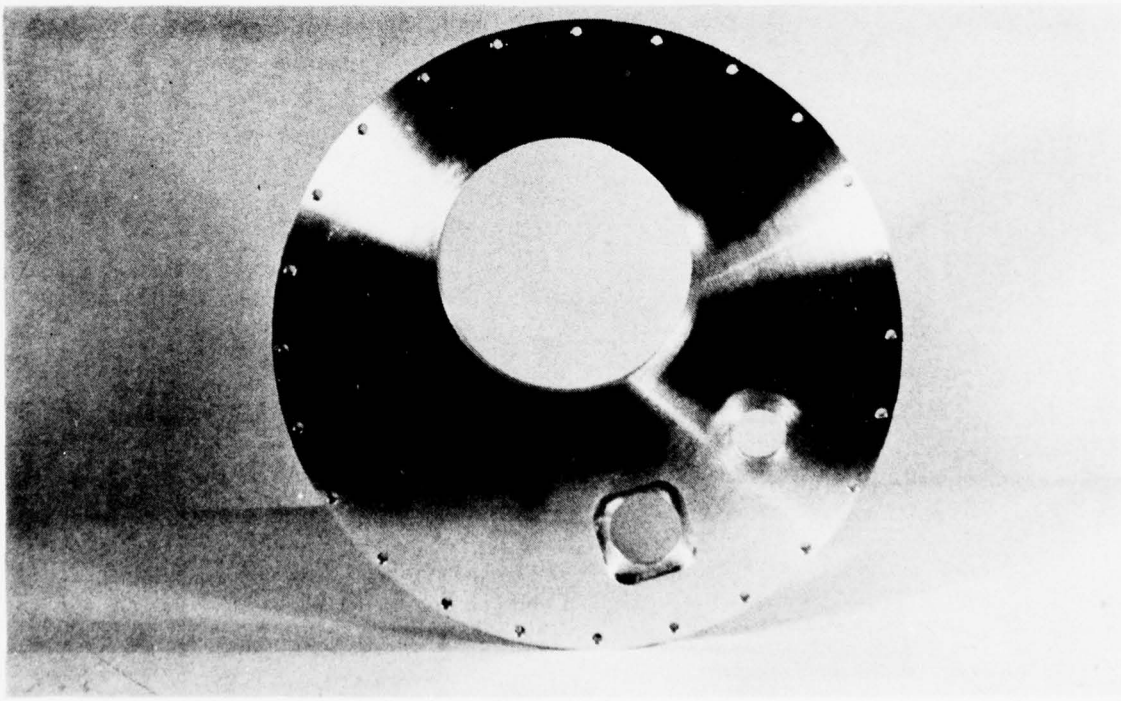

FIGURE 11
FRONT END COVER

temperature embrittlement qualities to which other metals are subject and also because its thermal conductivity is lower than that of most other metals.

The concept of the lobes between the inner fiberglass piece and the triangular shaped support pin is to minimize the heat path area.

3.7 Low Temperature Insulating Trunnion Support

A low heat leak support is required to bridge the vessel's warm wall ($300^{o}K$) and the front end of the shield (50^{o} to 77^{o} K). Unlike the support device in 3.6, the shield is supported through four (4) typical mechanical devices consisting mainly of a wire rope assembly and stacks of belleville spring washers, the principal parts of the assembly. The wire rope, a product of American Chain and Cable Company, Pennsylvania, is 1/16 inch in diameter, 7 X 7 strands and constructed of type 304 stainless steel with a double ball shank swaged on each end. The wire rope has a minimum breaking strength of 480 pounds, (Ref. 1). The belleville spring washers, B-0625-022S is a product of Associated Spring Corp, Connecticut. Their material is type 302 stainless steel and has a height of .022 inches and a 105 pound load at flat position, (Ref. 2). The washers are stacked two (2) in parallel and four (4) in series. The trunnion support is shown assembled to a gusseted upright member of the shield's cover. (See figures 12 & 13).

Anchoring the double shank ball and wire rope assembly between the shield and vessel through a stack of spring washers at one end and tension adjusting screw at the other, provides flexibility in the support. The support is assembled and adjusted until the rope is taut. (See figures 14 & 15). The ball and socket assembly of the trunnion joint on each end, allows the wire rope assembly to swivel freely as the shield shortens from thermal contraction. The wire rope is inclined approximately 5/32 inches to compensate for this thermal condition. (See figure 19, view "A").

Contraction in the wire rope assembly is caused by a thermal gradient across its extremity. This is compensated for by the compression of the belleville washers. A contraction of .003 inches was predicted in the wire rope assembly for a temperature change of 233^{o} K. A tension of 42.0 pounds (Ref. 2) in the wire rope results from the displacement of belleville washers caused by thermal contraction. The induced tension in the wire rope represents about 9 percent of the rope's breaking strength.

The heat contributed to the system through the trunnion support is largely dependent on the thermal resistances of the wire rope and belleville washers. From an analysis, it was found that the resistance of the belleville washer assembly represented 3½ percent of the wire rope's resistance. This would indicate that the resistance of the belleville washers is small compared to the wire rope and, therefore, can be neglected. With this hypothesis, the approximate heat leak through the support can be assumed to be dependent on the wire ropes resistance alone. From this, the total heat transmitted to the shield through the mechanical support devices is predicted to be approximately 278 milliwatts maximum. (See analysis in 5.8.3).

FIGURE 12

FWD. RADIATION SHIELD FRONT END COVER
WITH LOW TEMP. INSULATING SUPPORTS.

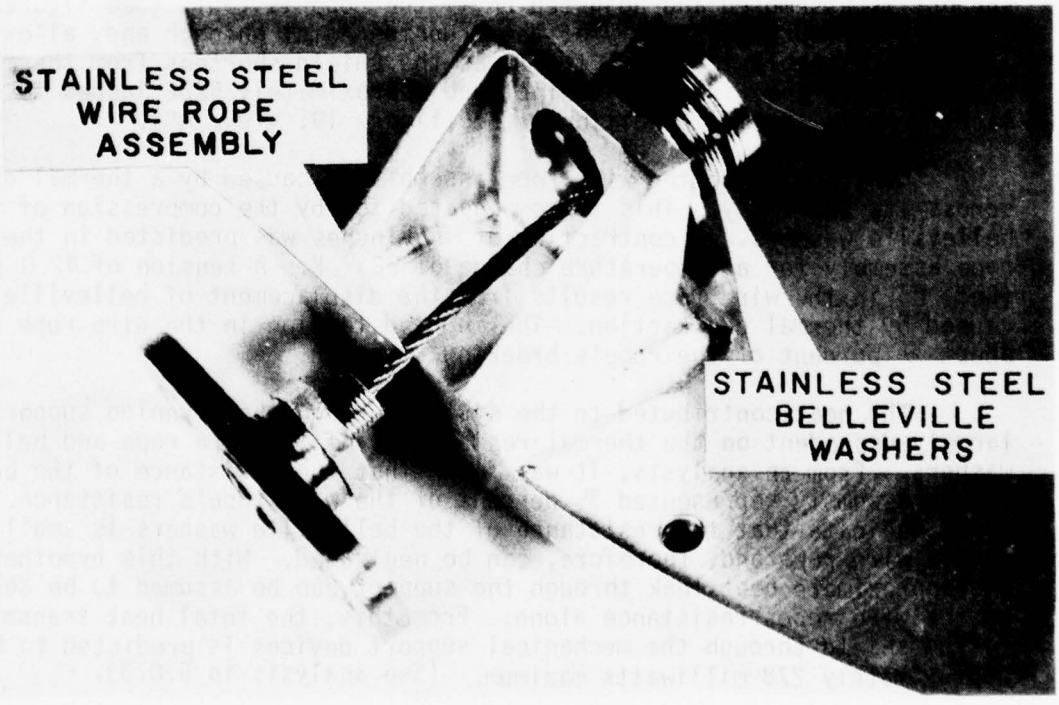

FIGURE 13

CLOSE UP OF THE LOW TEMP. INSULATING SUPPORT.

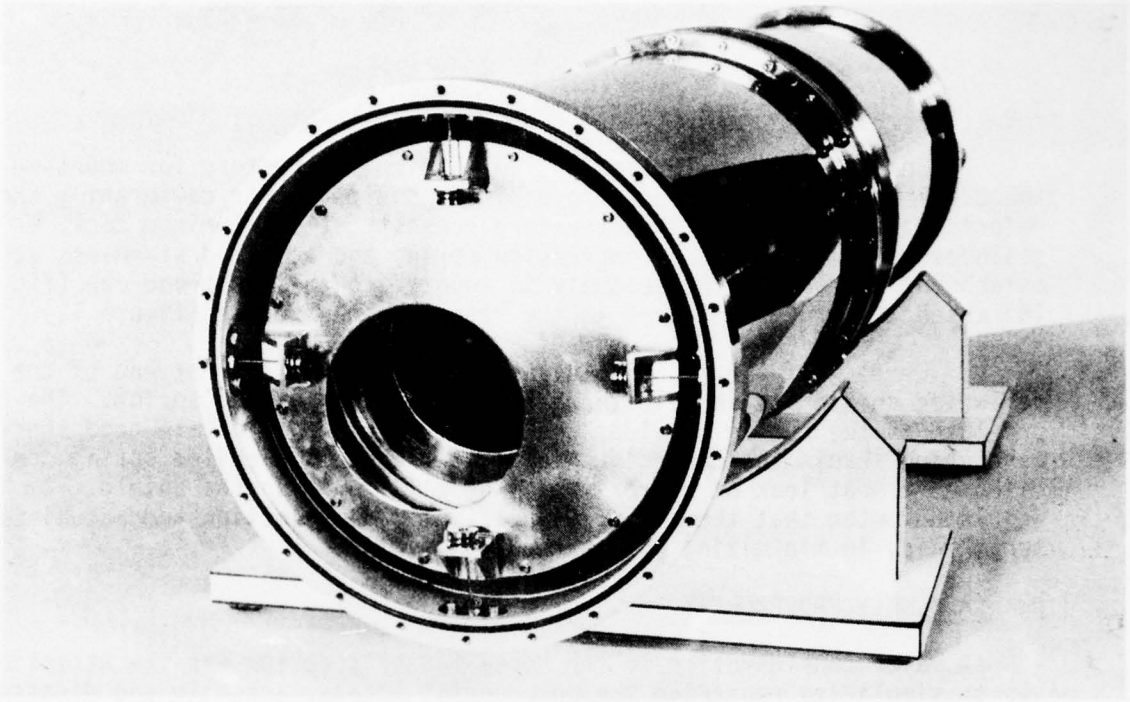

FIGURE 14

MODEL SENSOR — FRONT END COVER REMOVED
SHOWING ATTACHMENT OF LOW TEMP. INSULATING SUPPORTS

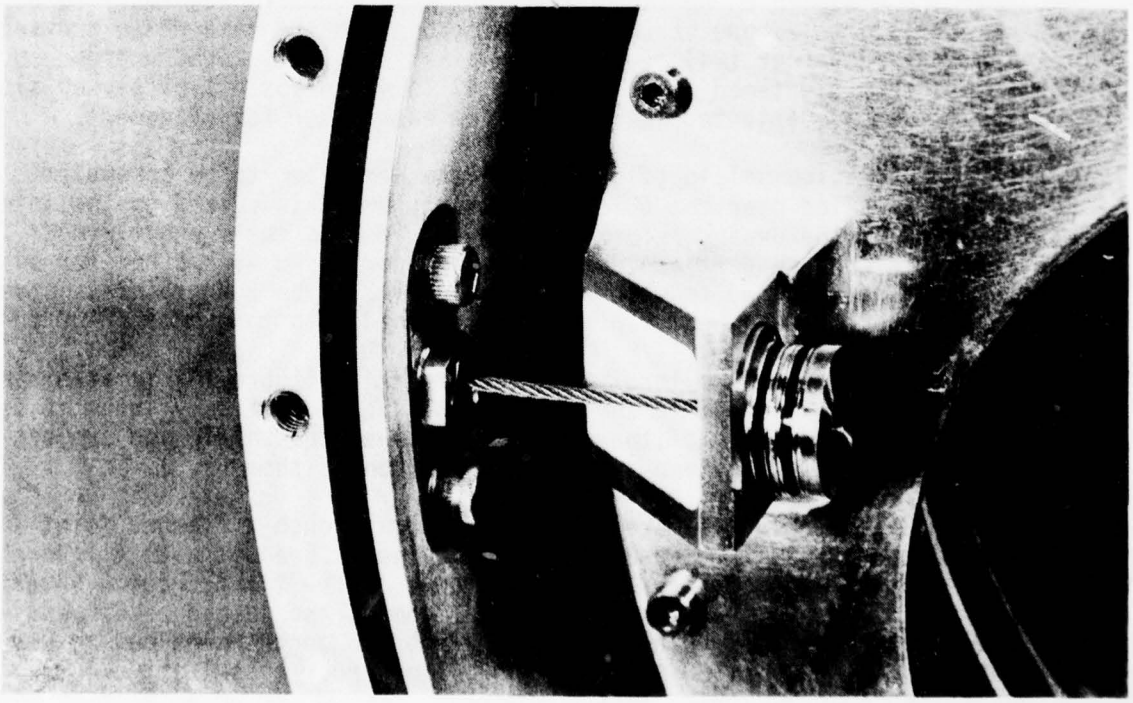

FIGURE 15

CLOSE UP VIEW SHOWING THE LOW TEMP.
INSULATING SUPPORT DEVICE IN ASSEMBLY

3.8 Black Body Source Mounting Structure

The device shown in figure 17 is a simple structure for mounting the black body source. The purpose of the source is for calibrating the detector's sensitivity. The structure consists of an aluminum deck, a stainless steel (type 340) compression spring and assorted stainless steel attachment hardward. The assembly is mounted to the front end cap (figure 16) which in turn is attached to the vessel's front cover (figure 11).

The deck of the mounting structure rests on the front end of the radiation shield and is held there by the pre-load in the spring. The pre-load in the spring provides the energy required to obtain good thermal conduction across the deck and shield interface. The coiled spring contributes a heat leak of approximately 40 milliwatts to the shield. It should be noted that the combination of material selection and actual spring length aids in minimizing the heat path losses.

4.0 ASSEMBLY PROCEDURE

A major consideration in the Model Sensor's design was the attention given to simplicity regarding the components' access, assembly and disassembly feasibility. The method of assembly presented in this section was the procedure used in the initial assembly phase and represented the best practical approach.

The dewar (figures 5 and 6) is seated on an assembly stool and establishes the basic foundation for the build-up of the model. The rear end plate is seated on the stool's top ring and locates the cold plate, support ring and rear end plate in an up-right position. The model is now ready to be assembled. The telescope structure is assembled to the cold plate and secured to it with twenty-four (24) type 304 stainless steel #10-24UNC unbrako socket head cap screws tightened to a torque of 40 to 45 in-lbs. Typical key slots in each member are oriented 180^{o} apart from each other for alignment.

The radiation shield (figure 7) is the next item to be assembled. The shield is installed over the telescope structure and is seated on the intermediate ring of the dewar, referred to in figure 6 as the support ring. Typical key slots in each part are oriented 180^{o} apart from each other for alignment. They are fastened together with twelve (12) type 304 stainless steel #8-32UNC unbrako socket head cap screws tightened to a torque of 28-30 in-lbs.

The low temperature insulating support ring (figure 10) is assembled to the forward end of the shield and simultaneously slides freely into the telescope structure. Because of the close fit between the shield and support ring, a slight pressure is required in the installation of them.

Two cylinder lengths are sealed together through a flanged joint and form the vacuum vessel. A #2-276 butyl "O"-Ring is greased with #11 Dow Corning Silicon Compound and installed into the groove of the flanged joint interface. The halves are dowel pinned together for alignment and joined with twenty-four (24) alloy steel, cadmium-plated #10-32UNF unbrako socket head cap screws tightened to a torque of 50 to 57 in-lbs. The vacuum vessel (figure 3) is now ready to be assembled to the dewar.

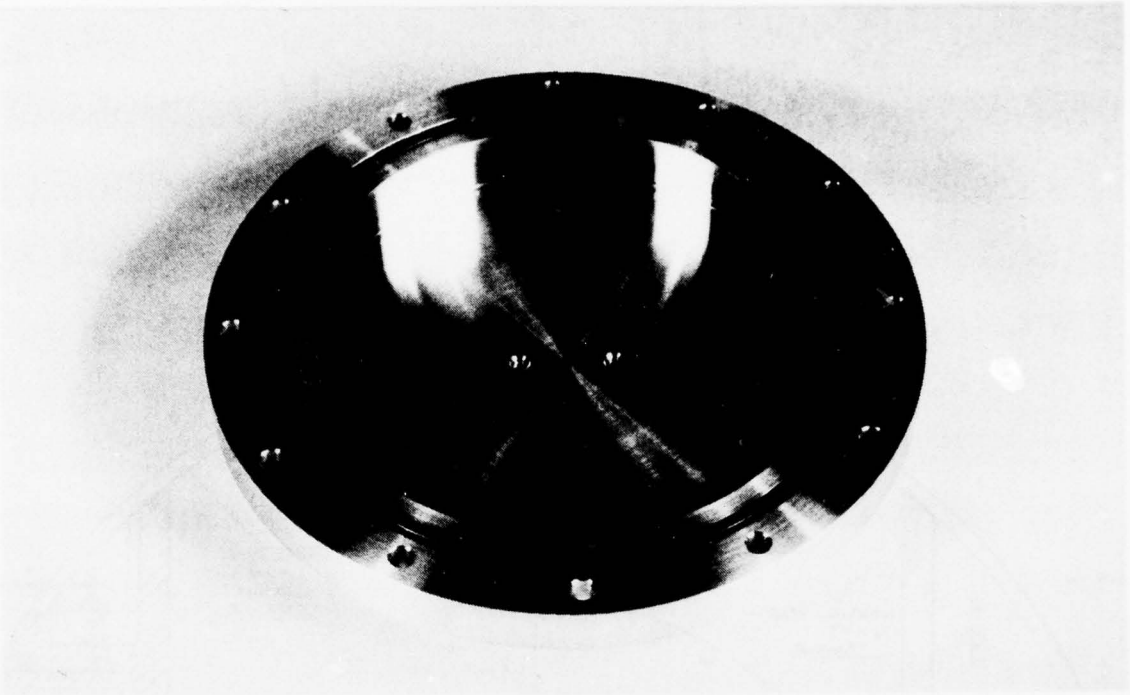

FIGURE 16
FRONT END CAP

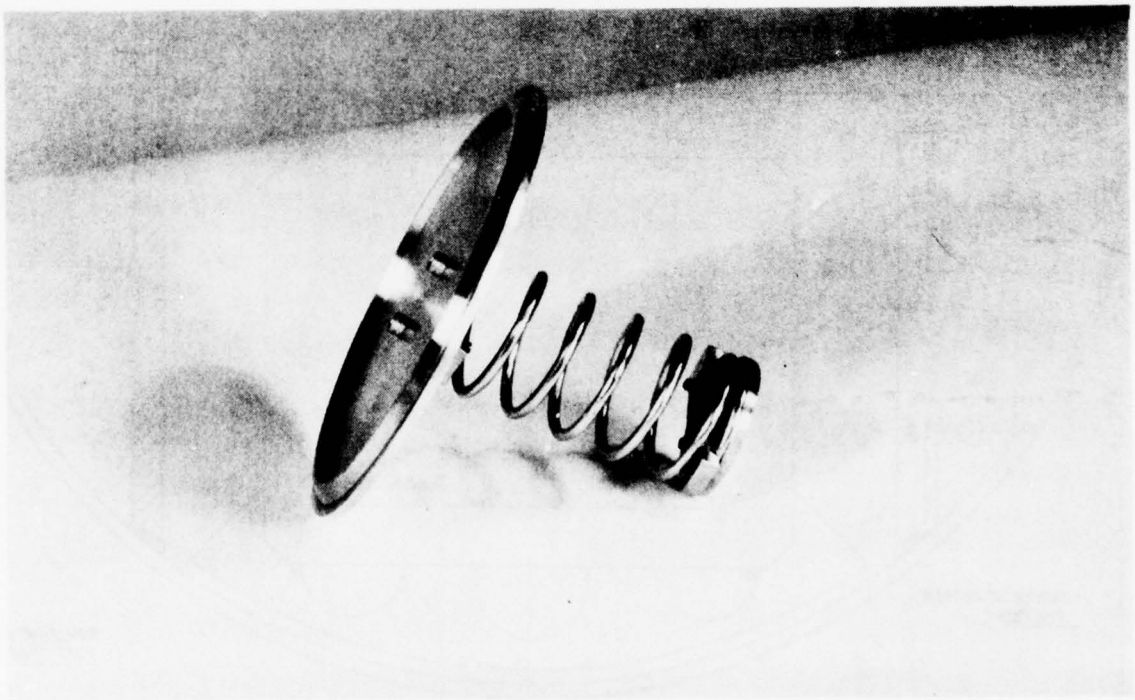

FIGURE 17
BLACKBODY SOURCE MTG. STRUCTURE

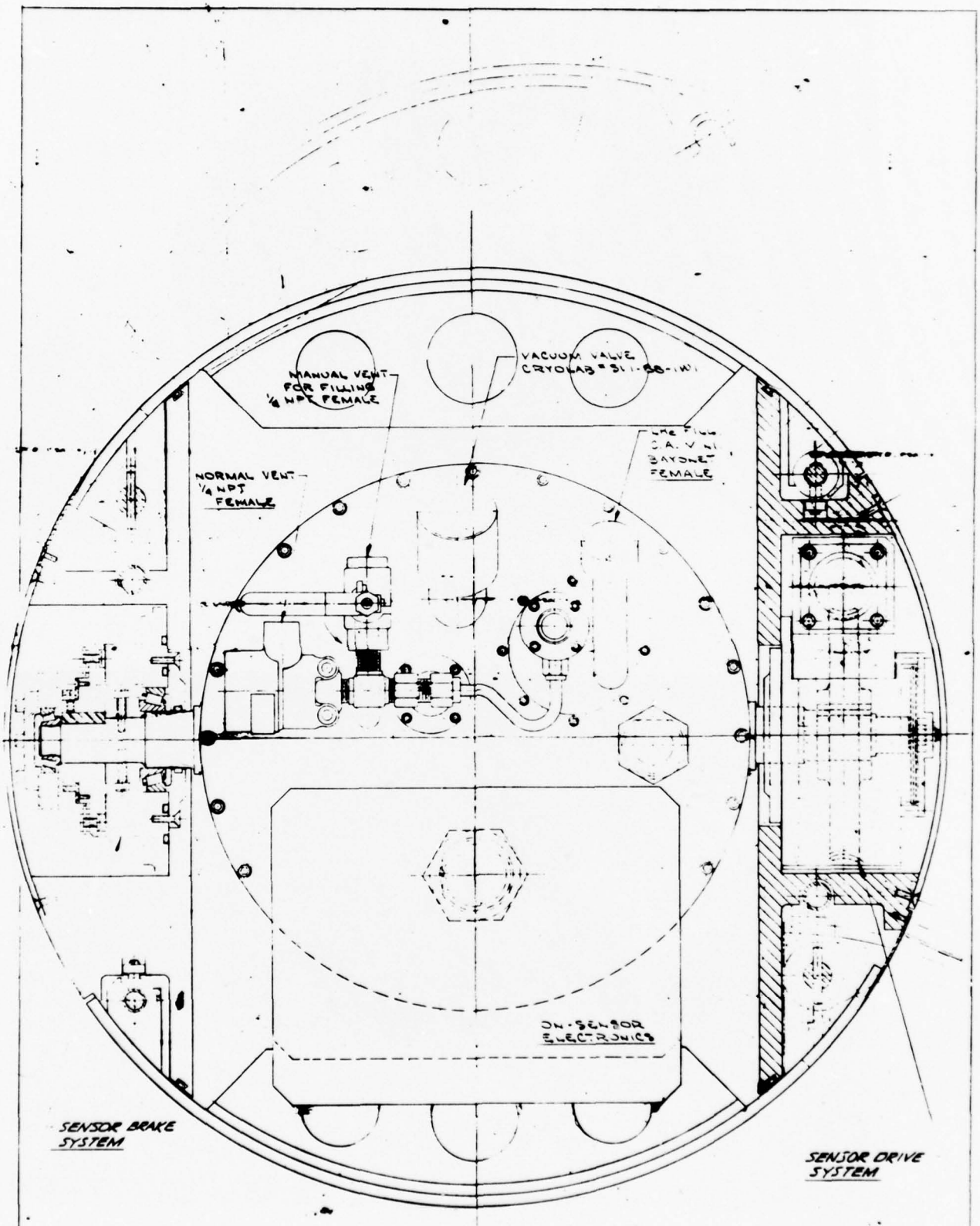

FIGURE 18.
PLAN VIEW OF SENSOR
AND PAYLOAD HOUSING

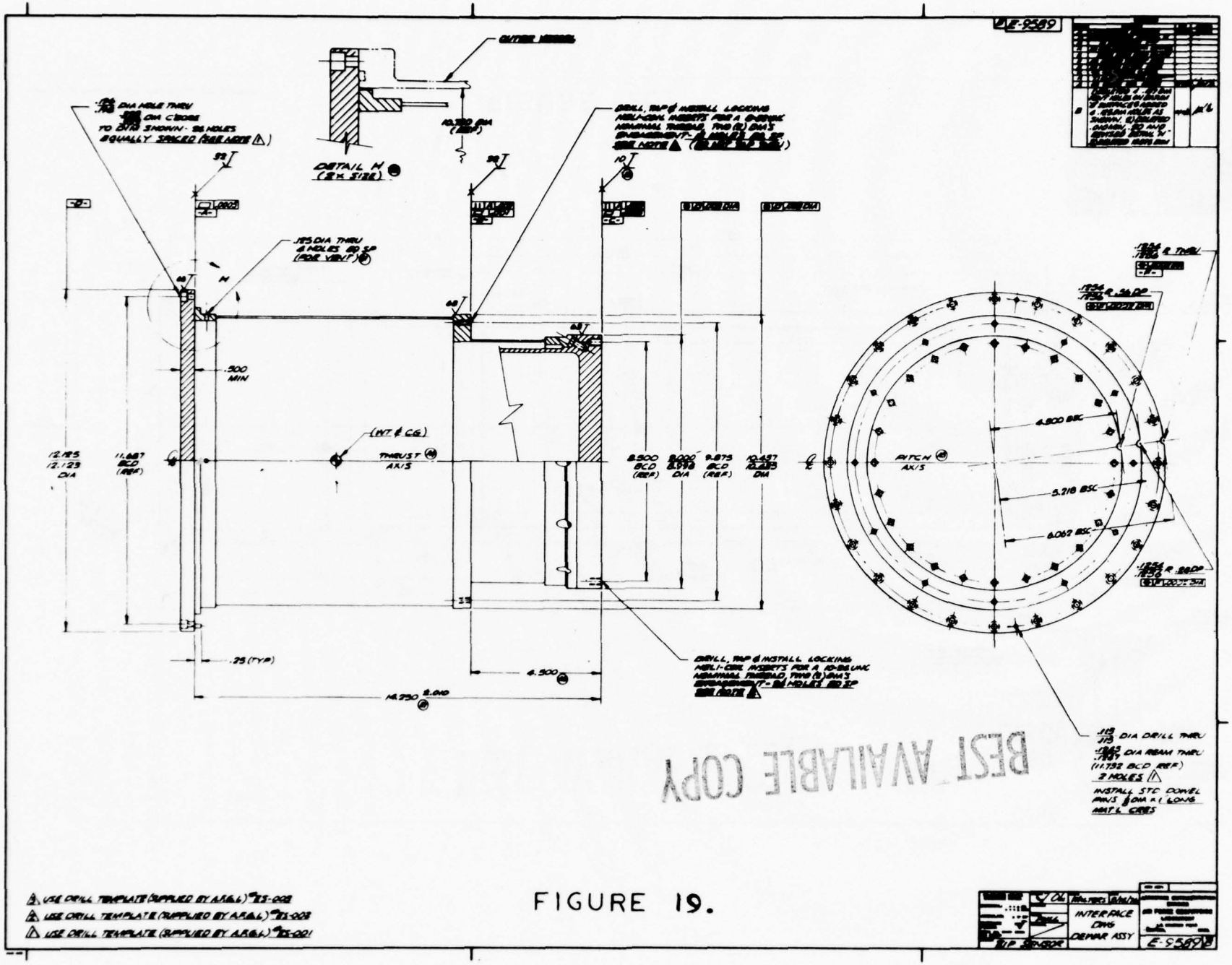

FIGURE 19.

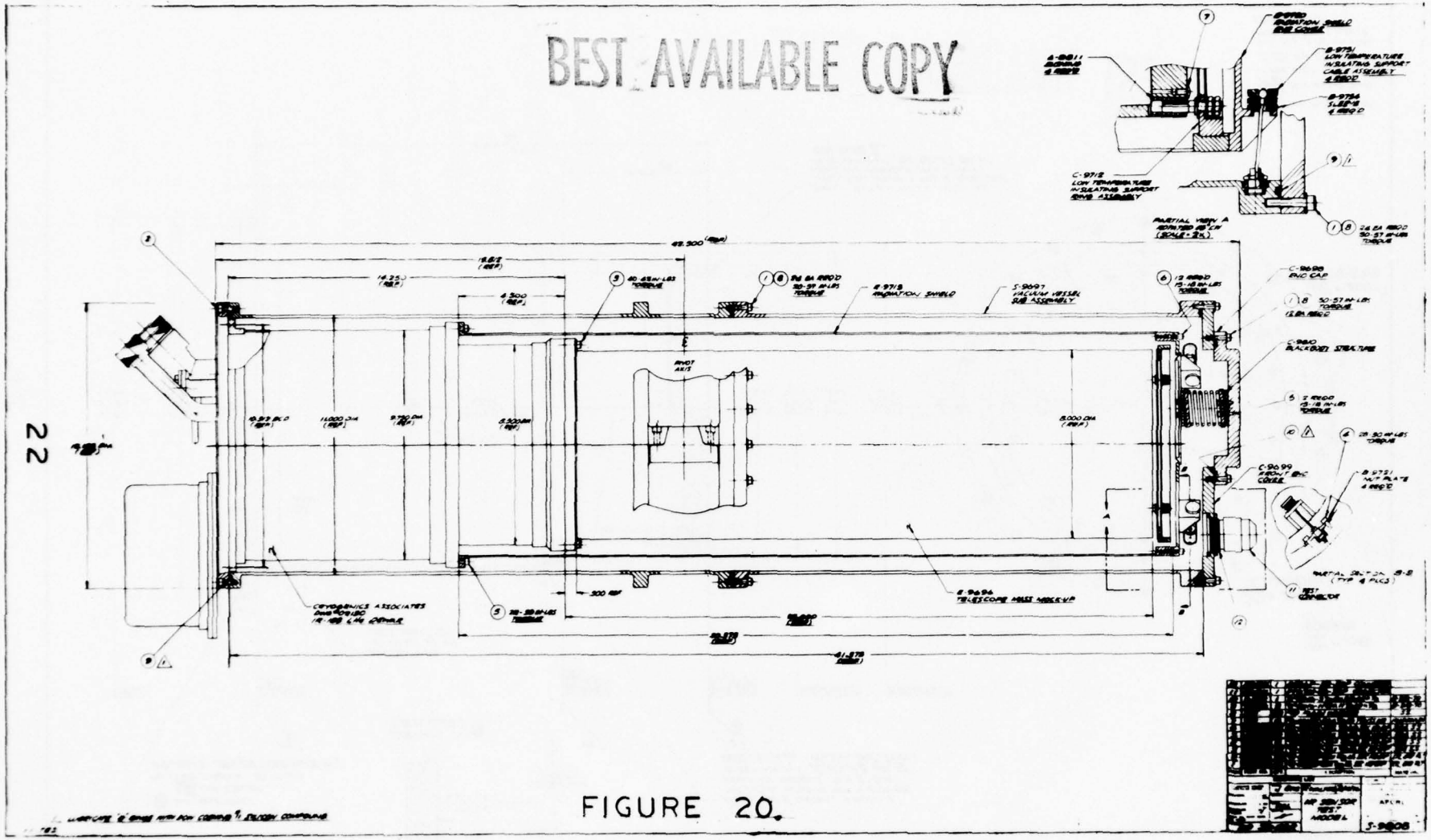

FIGURE 20.

An "O"-ring (#2-276, butyl) is greased and installed into the groove on the aft face end of the vessel. The vessel is carefully guided over the radiation shield and seated on the rear cover plate. Alignment is obtained by the engagement of dowel pins installed in the cover plate. The joint is bolted together with twenty-four (24) alloy steel, cadmium-plated #10-32UNF unbrako socket head cap screws tightened to a torque of 50 to 57 in-lbs.

The radiation shield cover and trunnion supports (figure 12) can now be assembled to the shield. The cover is aligned by positioning the eccentric hole in the cover 90^{o} from the gimbal axis and directly opposite the cryogen service hardware. Twelve (12) type 304 stainless steel #6-32UNC unbrako socket head cap screws are tightened to a torque of 15-18 in-lbs.

The insulating trunnion supports are now ready for mounting to the vessel. The attaching hardware (figure 13) should be directly in line with cavities in the vessel. The attaching plates, referred to in the design as nut plates, are inserted into the cavities and fastened (figures 14 and 15). After allowing slack in the cable, install two (2) each type 304 stainless steel #8-32UNC unbrako socket head cap screws and tighten to a torque of 28-30 in-lbs. The trunnion support is now adjusted until the cable is taut.

The front end cover (figure 11) is attached to the forward end of the vessel, enclosing the inner unit. An "O"-ring (#2-276, butyl) is greased and installed in the interface. The eccentric hole in the front cover is aligned over the eccentric hole in the shield's cover. The assembly is fastened together with twenty-four (24) alloy steel, cadmium-plated #10-32UNF unbrako socket head cap screws tightened to a torque of 50 to 57 in-lbs.

The front end cap (figure 16) and the black body source mounting structure (figure 17) are attached and make up the final unit to be assembled to the model. An "O"-ring (#2-252, butyl) is greased and installed into the groove on the end cap. The deck of the black body structure is inserted through the offset hole in the front cover and seated on the radiation shield cover. The cap is fastened to the front cover with twelve (12) alloy steel, cadmium-plated #10-32UNF unbrako socket head cap screws tightened to a torque of 50-57 in-lbs.

5.0 MECHANICAL DESIGN ANALYSIS

Initally, in the preliminary design phase, it was necessary to depend upon experience, design judgement and information from others, to properly proportion and construct the Model Sensor. This section presents the computations and results of the design analysis that followed the preliminary phase and deals with particular areas that were of concern. These particular areas are discussed in the design requirements, section 2.0, and represent the basic goals in the design (see figure 20).

ITEM	DESCRIPTION	w	d	(w)(d)
1	Vessel Front End Cover Plate	4.7	42.12	197.96
2	End Cap	1.7	42.88	72.90
3	Vacuum Vessel	24.5	21.00	515.00
4	Fwd. Radiation Shield	5.6	26.00	145.60
5	Fwd. Radiation Shield End Cover	0.6	40.75	24.45
6	Telescope Structure, Mass Mock-up	20.0	27.25	545.00
7	Focal Plane Detector (FPA)	0.3	15.88	4.76
8	Telescope Insulating Support Ring	0.5	40.25	20.12
9	Black Body Mounting Structure	0.3	41.88	13.82
10	Vessel Rear End Cover Plate	5.7	0.25	1.42
11	Liquid Helim Container, Filled	7.0	9.50	85.50
12	Dewar Insulating Support Stanchion	6.0	8.50	51.00
13	Cryogenic Hardware	2.5	(-) 2.00	(-) 5.00
14	On Sensor Electronics	4.0	(-) 2.00	(-) 8.00
TOTAL		83.4	-	1664

TABLE I.

WEIGHT AND CENTER OF GRAVITY- COMPUTATION RESULTS

5.1 System's Weight and Longitudinal Center of Gravity

The Model Sensor is a composite system of individual distributed bodies. A description of them is given in Table 1 with the computed results of their weights, distances from their mass centers with respect to the back of the vessel's rear cover, and moments. These results are approximate and are based on the assumption that the bodies are homogeneous.

The $\bar{z}$ coordinate locates the center of gravity on the longitudinal axis with respect to the back of the vessel's rear cover and is calculated using the summation of the results in Table 1. From the equation in Chapter VII of reference 3, the location of the center of gravity is

$$\bar{z} = \frac{\sum_{w\,d}}{\sum_{w}} = \frac{1664}{83.4} = 19.952 \text{ inches}$$

where w = weight of individual bodies, lbs.

d = perpendicular distance from the mass center of the individual bodies to the back of the vessel's rear cover, inches

The center of gravity of the system was positioned at 19.812 inches for manufacturing convenience.

5.2 System's Mass Moment of Inertia

The following method was employed in determining the system's mass moment of inertia. The mass moment of inertia is defined as the measure of resistance to rotational acceleration. The computed results of the system's individual bodies and the sum total of their inertias and products of the mass and square of the distances are recorded in Table 2. The computations are approximate and based on the same assumption made in section 5.1. The equations are given in Chapter VIII of reference 3.

The mass of the body (m_1) is given by

$$m_1 = \frac{w}{g} = \frac{4.7}{386} = .012 \text{ lbs-sec}^2/\text{in.}$$

where w = weight of body, 4.7 lbs from Table 1, Item 1

g = acceleration due to gravity, 386 in/sec^2

The masses, m_1 through m_{14} are typically computed and recorded in Column 2 of Table 2.

5.2.1 Item 1 - Vessel's Front End Cover

Size - 12 1/8" O.D x 6" I.D x 1/2" thick. The moment of inertia ($\bar{I}_1$) of the body with respect to a parallel axis through the mass center is given by

$$\bar{I}_1 = 1/4m(R^2 + r^2 + L^2/3) \qquad (3)$$

$$\bar{I}_1 = 1/4(.012)(6.06^2 + 3.0^2 + 0.5^2/3) = 0.14 \text{ lb-in-sec}^2$$

where

m = mass of body, .012 lbs-sec^2/in

R = outside radius, 6.06 inches

r = inside radius, 3.0 inches

L = Plate thickness, 0.5 inches

5.2.2 Item 2 - End Cap

Size - 6 1/2" O.D. x 4" I.D x 1 1/8" thick. From equation (3)

$$\bar{I}_2 = 1/4(.004)(3.25^2 + 2^2 + 1.12^2/3) = 0.015 \text{ lb-in-sec}^2$$

5.2.3 Item 3 - Vacuum Vessel

Size - 11" O.D. x 10 3/4" I.D x 41 3/8" long. From equation (3).

$$\bar{I}_3 = 1/4(.063)(5.5^2 + 5.38^2 + 41.38^2/3) = 9.92 \text{ lb-in-sec}^2$$

5.2.4 Item 4 - Fwd Radiation Shield

Size - 9 3/8" O.D. x 9 1/4" I.D. x 30 3/8" long. From equation (3).

$$\bar{I}_4 = 1/4(.014)(4.69^2 + 4.62^2 + 30.38^2/3)$$

$$\bar{I}_4 = 1.234 \text{ lb-in-sec}^2$$

5.2.5 Item 5 - Fwd Radiation Shield End Cover

Size - 9 1/2" O.D. x 4 1/2" I.D. x 1/8" thick. From equation (3).

$$\bar{I}_5 = 1/4(.001)(4.75^2 + 2.25^2 + .125^2/3)$$

$$\bar{I}_5 = 0.007 \text{ lb-in-sec}^2$$

5.2.6 Item 6 - Telescope Structure

Size - 8" O.D. x 7 1/2" I.D. x 25" long. From equation (3).

$$\bar{I}_6 = 1/4(.052)(4^2 + 3.75^2 + 25^2/3) = 3.112 \text{ lb-in-sec}^2$$

5.2.7 Item 7 - Focal Plane Detector

Size - 2" dia x 2" long. The detector was assumed to be a homogeneous mass. For a solid mass, the inertia is given by

$$\bar{I}_7 = 1/4mR^2 + 1/12mL^2 \qquad (4)$$

$$\bar{I}_7 = 1/4(.001)(1^2) + 1/12(.001)(2^2) = 0.001 \text{ lb-in-sec}^2$$

5.2.8 Telescope Insulating Support Ring

Size - 8 1/4" O.D. x 7 3/4" I.D. x 1/4" thick. From equation (3).

$$\bar{I}_8 = 1/4(.001)(4.125^2 + 3.875^2 + .25^2/3)$$

$$\bar{I}_8 = 0.008 \text{ lb-in-sec}^2$$

5.2.9 Black Body Mounting Structure

Size - 1 1/2" O.D. x 1 1/4" I.D. x 2" long. From equation (3).

$$\bar{I}_9 = 1/4(.001)(.75^2 + .62^2 + 2^2/3) = 0.001 \text{ lb-in-sec}^2$$

5.2.10 Vessel Rear End Cover

Size - 12 1/8" dia x 1/2" thick. For a solid plate the inertia is given by

$$\bar{I}_{10} = 1/4mR^2 \qquad (5)$$

$$\bar{I}_{10} = 1/4(.015)(6.06)^2 = 0.138 \text{ lb-in-sec}^2$$

5.2.11 Liquid Helium Container

Size - 8" O.D. x 7 3/4" I.D. x 11.5" long. From equation (3).

$$\bar{I}_{11} = 1/4(.018)(4^2 + 3.875^2 + 13.5^2/3)$$

$$\bar{I}_{11} = 0.340 \text{ lb-in-sec}^2$$

5.2.12 Dewar Insulating Support Assembly

Size - 10" O.D. x 9 3/4" I.D. x 13 1/2" long. From equation (3).

$$\bar{I}_{12} = 1/4(.015)(5^2 + 4.875^2 + 13.5^2/3)$$

$$\bar{I}_{12} = 0.411 \text{ lb-in-sec}^2$$

5.2.13 Cryogenic Hardware

A homogeneous bar, 4" dia x 4" long was assumed. From equation (4).

$$\bar{I}_{13} = 1/4(.006)(2^2) + 1/12(.006)(4^2)$$

$$\bar{I}_{13} = 0.014 \text{ lb-in-sec}^2$$

5.2.14 Item 14 - On Sensor Electronics

A homogeneous rectangular parallelepiped, 4" wide x 4" deep x 6" long. The inertia ($\bar{I}_{14}$) is given by

$$\bar{I}_{14} = 1/12m(a^2 + b^2) \qquad (6)$$

$$\bar{I}_{14} = 1/12(.01)(4^2 + 4^2) = 0.027 \text{ lb-in-sec}^2$$

where

a = width, 4 inches

b = depth, 4 inches

5.2.15 Results

From the parallel axis theorem and the computed results of the sum totals in Table 2, the mass moment of inertia (I) of the model sensor with respect to the longitudinal center of gravity is given by

ITEM	$\bar{I}$	m	d	d^2	md^2
1	0.140	.012	22.31	497.74	5.97
2	0.015	.004	23.07	532.22	2.31
3	9.92	.063	1.19	1.42	0.09
4	1.234	.014	6.19	38.31	0.54
5	0.007	.001	20.94	438.48	0.44
6	3.112	.052	7.44	55.35	2.88
7	0.001	.001	(-) 3.93	15.44	0.02
8	0.008	.001	20.44	417.79	0.42
9	0.001	.001	22.07	487.00	0.49
10	0.138	.015	(-)19.50	382.67	5.74
11	0.338	.018	(-)10.31	106.34	1.91
12	0.411	.015	(-)11.31	127.96	1.92
13	0.014	.006	(-)21.81	475.76	2.85
14	0.027	.010	(-)21.81	475.76	4.76
TOTAL	15.37	-	-	-	30.34

TABLE 2.

MASS MOMENT OF INERTIA - COMPUTATION OF RESULTS

$$I = \sum \bar{I} + \sum md^2 \tag{7}$$

$$I = 15.37 + 30.34 = 45.71 \text{ lb-in-sec}^2$$

where

$\sum \bar{I}$ = sum of the moments of inertia of the individual bodies, 15.37 lb-in-sec^2

$\sum md^2$ = sum of the products of the mass of the individual bodies and the square of the distance, 30.34 lb-in-sec^2

5.3 Vacuum Vessel Design

5.3.1 Vessel's Thickness

The minimum collapsing pressure (p_c) is given by the following expression, according to the ASME Code, referred to in Reference 4, p. 457:

$$p_c = (4)(1.27)p_a = (5)(15) = 75 \text{ psi} \tag{8}$$

where p_a is the allowable pressure (15 psi). The constant 4 is the required factor of safety, and the coefficient 1.27 is an out-of-roundness factor, which allows for the fact that the shell may not be exactly cylindrical.

The collapsing pressure for a short cylinder subjected to an external pressure (Ref. 4, p. 457) is given by

$$p_c = \frac{2.42E(t/D)^{5/2}}{(1-v^2)^{3/4}\left[(L/D)-0.45(t/D)^{1/2}\right]} \tag{9}$$

The shell's thickness (t) is then determined from the expression which is derived from equation (9), which gives

$$t = D\left[\frac{p_c(1-v^2)^{3/4}(L/D)}{2.42E}\right]^{2/5} \qquad (10)$$

$$t = 11.0\left[\frac{75(1-.334^2)^{3/4}(41.31/11)}{(2.42)(10.3 \times 10^6)}\right]^{2/5} = 0.112 \text{ in.}$$

A nominal size of 1/8 in. (0.125) was selected for the thickness of the vessel's wall. Substituting the nominal thickness into equation (9), the collapsing pressure is

$$p_c = \frac{(2.42)(10.3 \times 10^6)(.125/11.0)^{5/2}}{(1.-334)^{3/4}\left[(41.38/11.0)-0.45(.125/11.0)^{1/2}\right]} = 101 \text{ psi}$$

where

E = Young's modulus for aluminum 6061-T6, 10.3×10^6

t = Thickness of shell, .125 in.

D = Outside diameter of shell, 11.0 in.

v = Poisson's ratio for aluminum, .334

L = Unsupported length of shell, 41.38 in.

5.3.2 Thickness of Flat Heads

The thickness (t_h) of the vessel's flat head end closures which are bolted rigidly to the vessel's flanges and subjected to a uniform distributed external pressure (Ref. 5, p.449) is given by

$$t_h = d\sqrt{\frac{Kp_c}{S_{max}}} = 11.687\sqrt{\frac{(.162)(75)}{7,500}} = .470 \text{ in.} \qquad (11)$$

where

K = Constant Coefficient for a bolted head connection, 0.162

S_{max} = Maximum allowable stress for aluminum, 6061-T6 used in cryogenic vessel construction, 7,500 psi.

d = bolt circle diameter, 11.687 in.

p_c = collapsing pressure, 75 psi

A nominal size of 1/2 in. (.500) was selected for the head's thickness.

5.3.3 Vacuum Hold Time

Several various size B612-70 butyl rubber O-rings are used in the vacuum vessel assembly. A face type seal is used with grooves that provide 30% squeeze. The O-rings are lubricated with No.11 Dow Corning high vacuum grease to reduce leakage.

Butyl rubber was the material selected for the seals because it has excellent resistance to gas permeation, low outgassing characteristics and good resistance to compression set which makes it a particularly useful compound for vacuum applications.

The following computations are performed to find the approximate time (T) in hours for the pressure inside the vacuum vessel to rise from 10^{-5} torr to 10^{-4} torr due to a differential pressure of one (1) atmosphere acting across the seals.

The leak rate (L) of the O-ring seals is calculated from the following equation which is given in Reference 6, Section A2.

$$L = 0.7FDPQ(1-S)^2 \qquad (12)$$

where

F = permeability rate of butyl rubber, 0.2×10^{-8} std cc/sec/cm^2/cm at 75^0 F.

D = inside diameter of the O-rings,
(1) 11.0 in. diameter
(2) 5.25 in. diameter
(3) 1.625 in. diameter

P = pressure differential across the seal, 15 psi

Q = factor depending on percent of squeeze and whether the O-ring is lubricated or dry (from Ref.6, figure A2-3), 0.72 lubricated

S = Percent squeeze of the O-ring expressed as a decimal (30%), 0.3

Substituting the appropriate quantities in Equation (12), the leak rates of each O-ring seal is obtained as follows

$$L_1 = 3\left[(.7)(.2 \times 10^{-8})(11)(15)(.72)(1-.3)^2\right]$$

$$L_1 = 24.5 \times 10^{-8} cm^3/sec$$

$$L_2 = \left[(.7)(.2 \times 10^{-8})(5.25)(15)(.72)(1-.3)^2\right]$$

$$L_2 = 3.9 \times 10^{-8} cm^3/sec$$

$$L_3 = \left[(.7)(.2 \times 10^{-8})(1.625)(15)(.72)(1-.3)^2\right]$$

$$L_3 = 1.2 \times 10^{-8} cm^3/sec$$

The total leak rate is given by

$$L_T = L_1 + L_2 + L_3 \qquad (13)$$

$$L_T = 24.5 + 3.9 + 1.2 = 29.6 \times 10^{-8} cm^3/sec$$

where

L_1 = leak rate of the front, intermediate and aft vessel seals, $24.5 \times 10^{-8} cm^3/sec$

L_2 = leak rate of the front cap seal, $3.9 \times 10^{-8} cm^3/sec$

L_3 = leak rate of the Vac-Ion gauge seal, 1.2×10^{-8} cm^3/sec

In calculating the hold time, the vessel's volume of free air expressed in liters and the conversion of the total leak rate to torr-liter/sec. are needed.

The total leak rate expressed in torr-liter/sec is obtained by

$$L_T = (7.6 \times 10^{-1})(L_T cm^3/sec) \tag{14}$$

$$L_T = (7.6 \times 10^{-1})(29.6 \times 10^{-8})$$

$$L_T = 225 \times 10^{-9} \text{ torr-liter/sec}$$

where the multiplying quantity, 7.6×10^{-1} represents the conversion factor.

The volume of free air (V_f) is the net difference between the volume of the empty vessel and the volume of the sub-assembly mounted on the aft cover, inside the container. It was found that the vessel contained 2,730 cu.in. of free air, expressed in liters is

$$V_f = \frac{2,730}{61.023} = 44.74 \text{ liters} \tag{15}$$

The rate of pressure change in unit time is expressed by the following differential equation

$$\frac{dp}{dt} = \frac{L_T}{V_f} \tag{16}$$

from which

$$dp = \frac{L_T}{V_f} dt \tag{17}$$

Integrating Equation (17) the pressure is given by

$$P = \frac{L_T}{V_f} \int_{T_1}^{T_2} dt = \frac{L_T}{V_f} (T_2 - T_1) \qquad (18)$$

The change in time expression $(T_2 - T_1)$ in Equation (18) represents the time (T) for the pressure to change. Rearranging the terms in Equation (18) the time expressed in hours is given by

$$T = \frac{(V_f)(P)}{(3{,}600)(L_T)} \qquad (19)$$

Substituting the appropriate quantities in Equation (19) -- the time for the pressure (P) to rise from 10^{-5} to 10^{-4} torr in a vessel having a volume (V_f) of 44.74 liters and a leakage rate (L_T) of 225 x 10^{-9} torr-liter/sec is

$$T = \frac{(44.74)(10^{-4})}{(3{,}600)(225 \times 10^{-9})} = 5.5 \text{ hours}$$

5.4 Static Loading - Bending Moments and Load Reactions

This section presents a static load analysis on the flanged joints and support devices of the vessel's inner assembly and gives the approximate results of bending moments and load reactions. The inner assembly is attached to the vessel's aft cover and consists of a radiation shield, telescope housing, dewar and several supporting devices. The solution to the problem is simplified by assuming that the inner assembly is a composite construction consisting of two independent bodies, supported within one another. With this assumption, each body can be treated as a separate beam problem in solving for the load reactions and bending moments. The bending moments and load reactions acting on the assembly are caused by the combined loading of the bodies' mass and external applied forces. Discussions and computations for the independent bodies are presented in two separate case studies.

5.4.1 Case 1 - Inner Assembly body

In this case, the assembly is treated as a body of weight (Q_1) coupled with an external applied eccentric force (F) acting on the face of the supported end. The eccentric force is due to the energy stored in the compression spring of the black-body assembly (refer to the free body diagram in figure 21A). The problem is assumed to

resemble the combination of the conditions given in case 9, p.133 and Case 28, p.152 of Reference 7.

The resultant load reactions and bending moments R_1, R_2, M_1 and M_2 are given by the following expressions

$$R_1 = R_{1a} + R_{1b} \tag{20}$$

$$R_2 = R_{2a} + R_{2b} \tag{21}$$

$$M_1 = M_{1a} + M_{1b} \tag{22}$$

$$M_2 = M_{2a} + M_{2b} \tag{23}$$

where R_{1a}, R_{2a} and M_{1a} and M_{2a} represent the load reactions and bending moments due to the weight (Q_1); and R_{1b}, R_{2b}, M_{1b} and M_{2b} represent the load reactions and bending moments due to the eccentric force (F).

(Ref. 7, Case 9, p.133)

$$R_{1a} = \frac{Q_1 b^2}{2L^2}(2L + a) \tag{24}$$

$$R_{1a} = \frac{(40.5)(21.5)^2}{(2)(40.81)^3} 2(40.81) + 19.31$$

$$R_{1a} = 13.9 \text{ lbs}$$

where

Q_1 = weight of body, 40.5 lbs

b = distance of mass to fixed end, 21.5 in.

a = distance of mass to supported end, 19.31 in.

L = unsupported length, 40.81 in.

The load reaction at the fixed end (R_{2a}) due to (Q_1) is given by

$$R_{2a} = Q_1 - R_{1a} \tag{25}$$

$$R_{2a} = (40.5\text{-}13.9) = 26.6 \text{ lbs}$$

The bending moment at the fixed end (M_{1a}) due to (Q_1) is given by

$$M_{1a} = - \frac{Q_1 ab}{2L^2} (L + a) \tag{26}$$

$$M_{1a} = - \frac{(40.5)(19.31)(21.5)}{2(40.81)^2} (40.81 + 19.31)$$

$$M_{1a} = -304 \text{ in.-lbs}$$

The bending moment at the radiation shield joint (M_{2a}) due to (Q_1) is given by

when $x > a$

$$M_{2a} = R_{1a} x - Q_1 (x-a) \tag{27}$$

$$M_{2a} = (13.9)(31.06)\text{-}40.5(31.06\text{-}19.31)$$

$$M_{2a} = -44.1 \text{ in.-lbs}$$

where

x = distance of radiation shield joint from supported end, 31.06 in.

The load reaction at the supported end (R_{1b} and R_{2b}) due to (F) is given by the equation

(Ref. 7, Case 28, p.152)

$$-R_{1b} = R_{2b} = \frac{3M}{2L} \tag{28}$$

The moment (M) is given by the equation

$$M = Fd \tag{29}$$

Substituting Equation (29) for M in (28) gives

$$-R_{1b} = R_{2b} = \frac{3Fd}{2L} \tag{30}$$

$$-R_{1b} = R_{2b} = \frac{(3)(32.5)(1.5)}{(2)(40.81)} = 1.8 \text{ lbs}$$

where

F = eccentric force, 32.5 lbs

d = eccentricity, 1.5 in.

L = unsupported length, 40.81 in.

The bending moment at the fixed end (M_{2b}) due to (F) is given by

$$M_{1b} = -\frac{Fd}{2} \tag{31}$$

$$M_{1b} = -\frac{(32.5)(1.5)}{2} = -24.4 \text{ in.-lbs}$$

The bending moment at the radiation shield joint (M_{2b}) due to (F) is given by

$$M_{2b} = \frac{Fd}{2L}(2L-3x) \qquad (32)$$

$$M_{2b} = \frac{(32.5)(1.5)}{(2)(40.81)}\left[(2)(40.81)-(3)(31.06)\right]$$

$$M_{2b} = -6.9 \text{ in.-lbs}$$

from Equation (20)

$$R_1 = R_{1a} + R_{1b}$$

$$R_1 = (13.9 - 1.8) = 12.1 \text{ lbs}$$

from Equation (21)

$$R_2 = R_{2a} + R_{2b}$$

$$R_2 = (26.6 + 1.8) = 28.4 \text{ lbs}$$

from Equation (22)

$$M_1 = M_{1a} + M_{1b}$$

$$M_1 = (-304-24.4) = -328 \text{ in.-lbs}$$

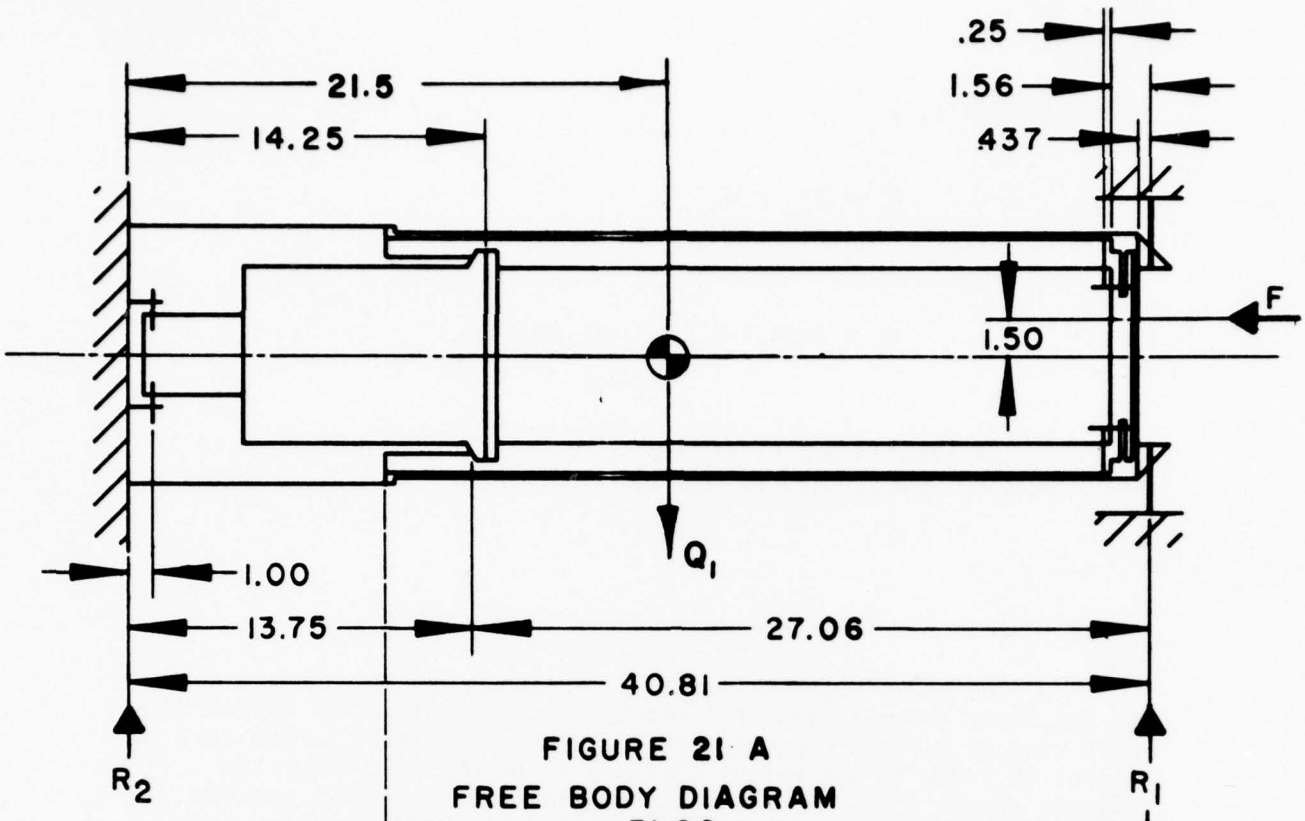

FIGURE 21 A
FREE BODY DIAGRAM

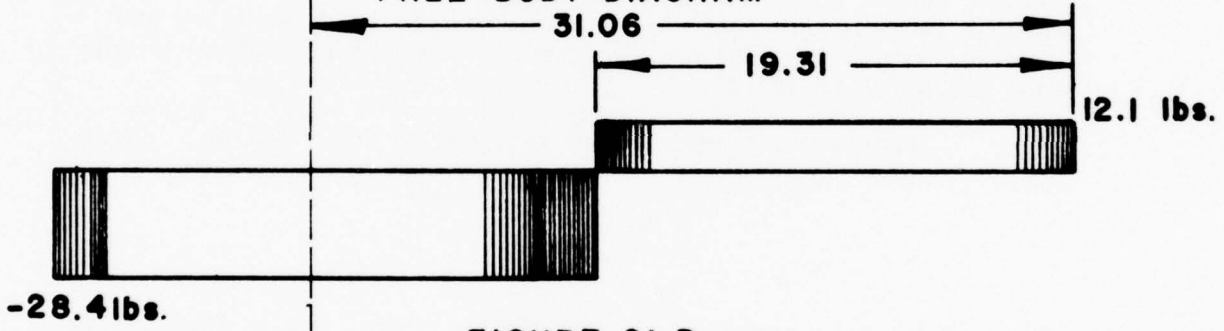

FIGURE 21 B
SHEAR DIAGRAM

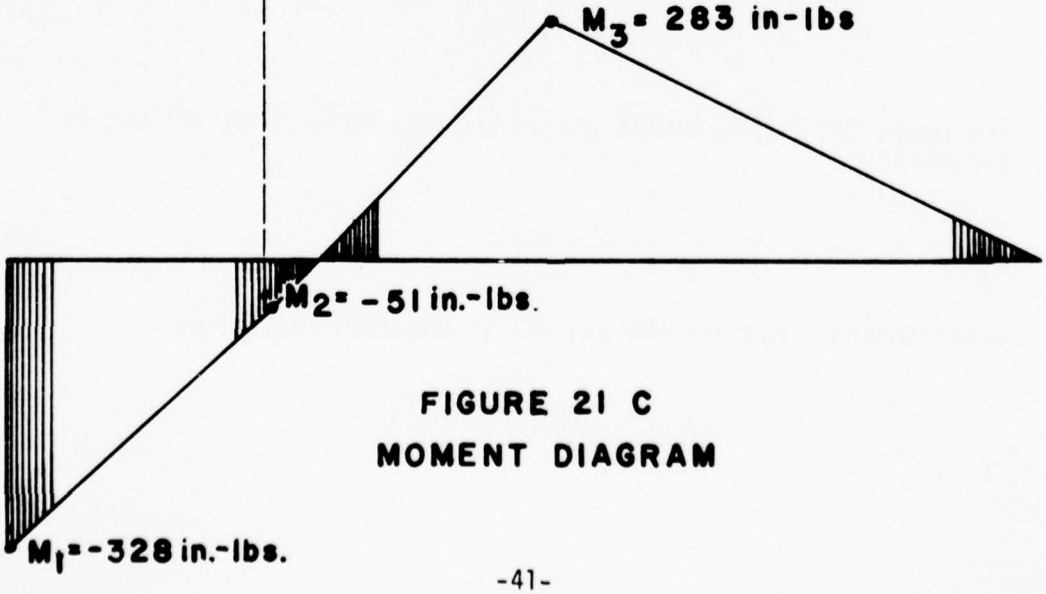

FIGURE 21 C
MOMENT DIAGRAM

from Equation (23)

$$M_2 = M_{2a} + M_{2b}$$

$$M_2 = (-44.1-6.9) = -51 \text{ in.-lbs}$$

The results are plotted on a shear diagram in figure 21B and a bending moment diagram in figure 21C.

5.4.2. Case 2 - Telescope Housing and Dewar Assembly

The body shown in figure 22A is supported at each end within the inner assembly and is fixed to it at the radiation shield support ring by a rigid support tube. It is assumed that a resultant moment (M_o) due to the weight (Q_2) and force (F) acts about the elastic center (EC), the point on the line which is shown passing through the support ring. The computations of load reactions and bending moments that follow are based on a manner of loading similar to Case 32, p.152 of Ref.7).

The resultant moment (M_o) is given by the equation

$$M_o = M_a - M \tag{33}$$

where (M_a) is the moment about the elastic center due to (Q_2) and is given by

$$M_a = (Q_2)(d_2) \tag{34}$$

and where (M) is the moment due to the eccentric force (F) and is expressed by

$$M = (F)(d) \tag{35}$$

substituting Equations (34 and 35) in Equation (33) gives

$$M_o = (Q_2)(d_2) - (F)(d)$$

from which

$$M_o = (29.5)(11.78)-(32.5)(1.5)$$

$$M_o = 298.76 \text{ in.-lbs}$$

where

Q_2 = weight of body, 29.5 lbs

d_2 = distance from the elastic center to the weight of body, 11.78 in.

F = eccentric force, 23.5 lbs

d = eccentricity, 1.5 in.

The load reactions and bending moments designated by R_3, R_4, $M_{max(+)}$, $M_{max(-)}$ and M are given by the following expressions, (Case 32, p.156 of Ref. 7).

$$R_3 = \frac{M_o}{L} \tag{36}$$

$$-R_4 = \frac{M_o}{L} \tag{37}$$

$$M_{max(+)} = R_4 a + M_o \tag{38}$$

$$M_{max(-)} = R_4 a \tag{39}$$

$$M = R_4 x + M_o \tag{40}$$

The load reaction (R_3) at the front end is given by Equation (36)

$$R_3 = \frac{M_o}{L}$$

from which

$$R_3 = \frac{298.76}{38} = 7.9 \text{ lbs}$$

The load reaction (R_4) at the aft end is given by Equation (37)

$$R_4 = - \frac{M_o}{L}$$

from which

$$R_4 = - \frac{298.76}{38} = -7.9 \text{ lbs}$$

The maximum (positive) bending moment ($M_{max(+)}$) at the support ring is given by Equation (38)

$$M_{max(+)} = R_4 a + M_o$$

from which

$$M_{max(+)} = (-7.9)(8.5) + 298.76$$

$$M_{max(+)} = 323 \text{ in.-lbs}$$

The maximum (negative) bending moment ($M_{max(-)}$) at the support ring is given by Equation (39)

$$M_{max(-)} = R_4 a$$

from which

$$M_{max(-)} = (-7.9)(8.5) = -67 \text{ in.-lbs}$$

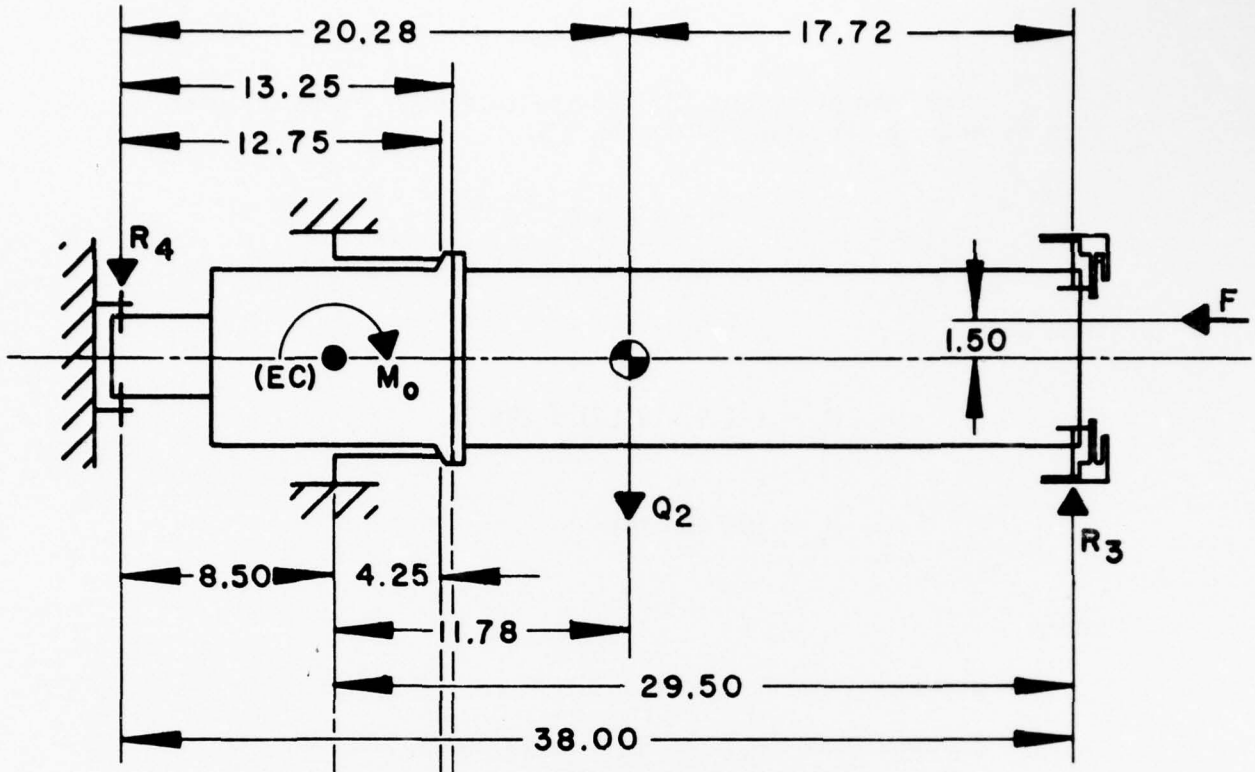

FIGURE 22A
FREE BODY DIAGRAM

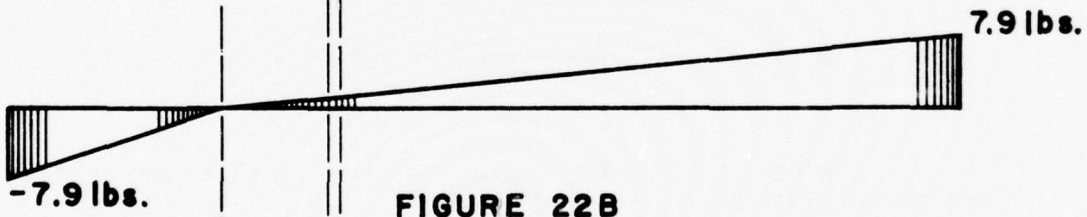

FIGURE 22B
SHEAR DIAGRAM

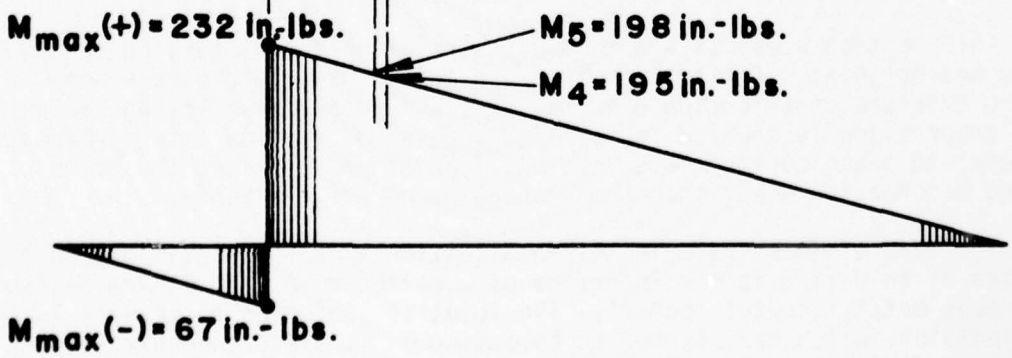

FIGURE 22C
MOMENT DIAGRAM

The bending moment (M_4) at the telescope to dewar interface is given by Equation (40) when $x > a$

$$M = R_4 x + M_o$$

from which

$$M_4 = (-7.9)(13.25) + 298.76$$

$$M_4 = 195 \text{ in.-lbs}$$

where

x = distance from (R_4) to the interface, 13.25 in.

a = distance from (R_4) to the Elastic Center, 8.5 in.

The bending moment (M_5) at the support tube to dewar interface is also given by Equation (40)

when x = 12.75

$$M_5 = (-7.9)(12.75) + 298.76 = 198 \text{ in.-lbs}$$

The results are plotted and indicated on shear and bending moment diagrams in figures 22B and 22C.

5.5 Distortion - Vessel's Rear Vacuum Seal Joint

This section presents a method of calculating the distortion in the vacuum sealed joint. Distortion of sealed joints usually causes a non-uniform pressure distribution over the seal which can cause leakage at points where compression is too low for sealing. Joint distortion exists whenever the metal to metal contact faces are not flat or parallel and the bolts undergo deformation other than that caused by normal tightening.

The type of joint used in this application is a face seal joint which consists of an O-ring in the interface of a bolted cover and flange assembly that makes metal to metal contact. The joint is subjected to several loading conditions which are assumed to be acting on it simultaneously. The loading conditions are as follows:

1) a uniform external load of 15 psi acting over the entire surface of the cover,

2) a uniform O-ring pressure of 15 lbs/linear in. (Ref. 6, p.A4-8) acting on a concentric circular ring,

3) a 100g longitudinal acceleration load acting on a concentric circular ring, and

4) a central couple acting on the cover due to a 100g lateral acceleration load.

The analysis that follows is based on the assumptions that:

1) the flange of the vessel is stable for each loading condition, and

2) the distortion in the joint occurs from the cover bowing and elongation in the bolts.

Calculations are performed for each manner of loading using equations from cases given in Table X of Ref. 8.

5.5.1 Loading Condition 1 - External Pressure

Determine the deflection (y_{q1}) at the O-ring and tension in the bolts (F_{b1})

Assuming a fixed edge condition for the support of the cover (Figure 23) and using the equations for case 6, Ref. 8 - the maximum deflection (y_{max}) at the center of the cover for a uniform external pressure over the entire surface is given by

$$y_{max} = - \frac{3w\pi a^2 \left[(1/v)^2 - 1\right] a^2}{16\pi E (1/v)^2 t^3} \qquad (41)$$

$$y_{max} = - \frac{(3)(15)(5.375)^2 \left[(1/.334)^2 - 1\right] 5.375^2}{(16)(10.3 \times 10^6)(1/0.334)^2 (0.5)^3}$$

$$y_{max} = -.00162 \text{ in.}$$

where

E = Young's modulus for 6061-T6 aluminum, 10.3 x 10^6

v = Poisson's ratio for aluminum, 0.334

a = inside radius of vessel, 5.375 in.

t = thickness of cover, 0.5 in.

w = external pressure, 15 psi

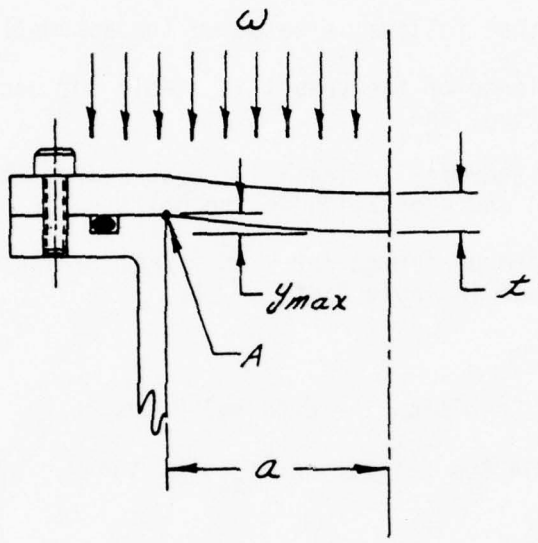

Figure 23 - Flanged joint,
Uniform external pressure over entire surface
of cover

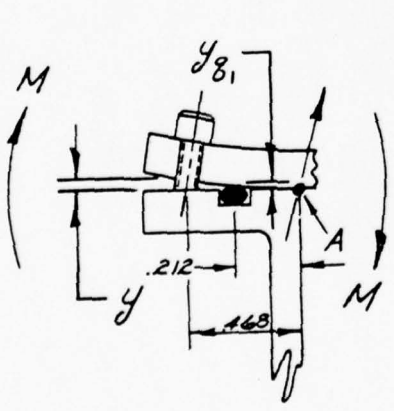

Figure 24a - Flanged joint,
cover distortion due
to bolt elongation

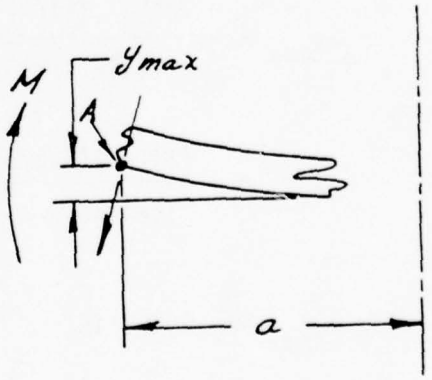

Figure 24b - Flanged joint,
bowing due to
external pressure

Now, assuming that the clamped cover shown in Figure 23 is a flexible connection and not fixed as previously assumed, then elongation in the bolts due to the uniform edge moment in the plate from bowing can cause the cover to separate from the seal. This condition is shown exaggerated in Figure 24a and 24b.

The problem is simplified by separating the cover at point "A" into two parts

1) a ring supported at the inner edge with a uniform moment along the outer edge (Figure 24a)

2) a plate, unsupported, with a uniform edge moment (Figure 24b).

Using the equations for Case 12, Ref. 8, the maximum deflection of the unsupported plate shown in Figure 24b is expressed by

$$y_{max} = - \frac{6\left[(1/v)-1\right] Ma^2}{E(1/v)t^3} \qquad (42)$$

Rearranging the terms in Equation (42) and solving for the moment (M) in terms of (y_{max}) gives

$$M = - \frac{E(1/v)}{6\left[(1/v)-1\right] a^2} (y_{max})(t^3) \qquad (43)$$

Substituting (y_{max}) from equation (41) into (43) and assuming that they are equal gives

$$M = - \frac{(10.3 \times 10^6)(1/0.334)}{6\left[(1/0.344)-1\right] 5.375^2} (-0.00162)(0.5)^3$$

$$M = 18 \text{ in.-lbs}$$

Assuming the edge moment (M) in the plate and ring are equal and the bolts are equally loaded, then the tension in the bolts (F_{b1}) can be calculated by

$$F_{b1} = \frac{M}{d} = \frac{18}{0.468} = 38.5 \text{ lbs} \qquad (44)$$

where

d = distance from point "A" to the bolt's center, 0.468 in.

The bolt elongation (y) is given by the formula

$$y = \frac{F_{b1}L}{AE} = \frac{(38.5)(.625)}{(.020)(30 \times 10^6)} \qquad (45)$$

$$y = 4 \times 10^{-5} \text{ in.}$$

where

L = length of bolt, 0.625 in.

E = Young's modulus for steel, 30×10^6

A = Cross Sectional area for the threaded portion of a #10-32 bolt, 0.020 $in.^2$

Solving for (y_{q1}) by similar triangles (Fig.24a) gives

$$y_{q1} = \frac{(.212)(4 \times 10^{-5})}{.468} = 1.8 \times 10^{-5} \text{ in.}$$

The amount of distortion in the cover at the O-ring seal due to the vacuum in the container is 1.8×10^{-5} inches. The tension in each bolt is 38.5 pounds.

5.5.2 Loading Condition 2 - O-ring Compression

Determine the deflection (y_{q2}) at the O-ring and tension in the bolts (F_{b2}) for a uniform load of 15 lbs/linear in. acting on a concentric circular ring of the cover (Fig. 25)

Assuming a fixed edge condition for the support of the cover and using the equations for Case 8, Ref. 8, the deflection (y_{q2}) in the cover is given by

$$y_{q2} = \frac{3\pi 2r_o w \left[(1/v)^2 - 1\right]}{2\pi E(1/v)^2 t^3} \left[\frac{1}{2}(1 + \frac{r_o^2}{a^2})(a^2 - r_o^2) - 2r_o^2 \ln\frac{a}{r_o}\right] \qquad (46)$$

from which

$$y_{q2} = \frac{(3)(2)(5.587)(15)\quad\left[(1/.334)^2-1\right]}{(2)(10.3 \times 10^6)(1/.334)^2(.5)^3}$$

$$\left[\frac{1}{2}(1 + \frac{5.587^2}{5.843^2})(5.843^2 - 5.587^2) - 2(5.587)^2 \ln\frac{5.843}{5.587}\right]$$

$$y_{q2} = 0.065 \times 10^{-5} \text{ in.}$$

where

E = Young's modulus for 6061-T6 aluminum, 10.3×10^6

v = Poisson's ratio for aluminum, 0.334

a = radius of bolt circle, 5.843 in.

r_o = mean radius of O-ring and applied load, 5.587 in.

t = thickness of cover, 0.5 in.

w = unit loading, 15 lbs/linear in.

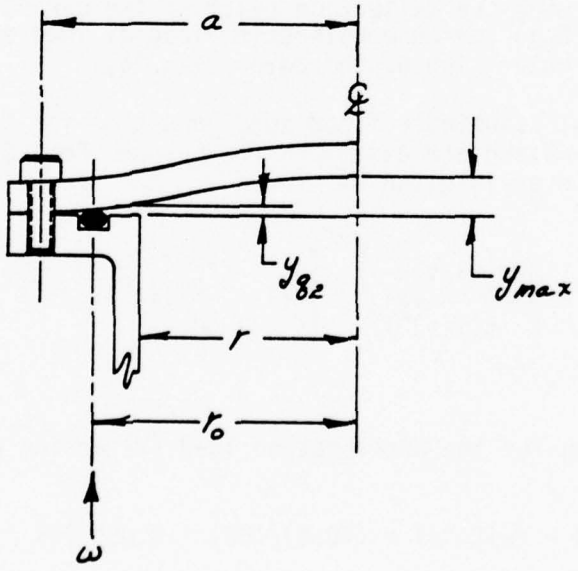

Figure 25 - Flanged Joint, cover distortion due to O-ring compression

Assuming the bolts are equally loaded by the compression of the O-ring on the cover, then the tension in the bolts is

$$F_{b2} = \frac{\pi 2 r_o w}{n} = \frac{(3.14)(2)(5.587)(15)}{24} \qquad (47)$$

$$F_{b2} = 22 \text{ lbs}$$

where

w = unit load 15 lbs/in.

r_o = mean radius of O-ring, 5.587 in.

n = number of bolts, 24

The amount of distortion in the cover at the O-ring seal due to O-ring compression is 0.065×10^{-5} inches and the bolt tension is 22 pounds

5.5.3 Loading Condition 3 - Longitudinal Acceleration

Determine the deflection (y_{q3}) at the O-ring and tension in the bolts (F_{b3}) for an acceleration load of 100g's acting on a concentric circular ring of the cover (Fig.26).

Again, assuming a fixed edge condition for the support of the cover. Using the equations for Case 8, Ref. 8, the deflection (y_{q3}) in the cover is given by

$$y_{q3} = \frac{3W\left[(1/v)^2-1\right]}{2\ E(1/v)^2 t^3}\left[\frac{1}{2}(1+\frac{r_o^2}{a^2})(a^2-r^2)-(r^2+r_o^2)\ln\frac{a}{r}\right] \qquad (48)$$

Solving for the acceleration load (W) acting on the cover

$$W = (w)(g's) = (40.5)(100) = 4{,}050 \text{ lbs} \qquad (49)$$

where

w = weight of the inner assembly attached to the cover, 40.5 lbs

g's = acceleration force, 100 g's

Substituting (W) into Equation (48) the deflection is

$$y_{q3} = \frac{(3)(4{,}050)\left[(1/.334)^2-1\right]}{(2)(3.14)(10.3 \times 10^6)(1/.334)^2(.5)^3}$$

$$\left[\frac{1}{2}\left(1 + \frac{5.156^2}{5.843^2}\right)(5.843^2 - 5.587^2) - (5.587^2 + 5.156^2)\ln\frac{5.843}{5.587}\right]$$

$$y_{q3} = 1.7 \times 10^{-5} \text{ in.}$$

where

r_o = radius of applied load, 5.156 in.

r = mean radius of O-ring, 5.587 in.

a = radius of bolt circle, 5,843 in.

t = thickness of cover, .5 in.

v = Poisson's ratio for aluminum, .334

E = Young's modulus for 6061-T6 aluminum, 10.3×10^6

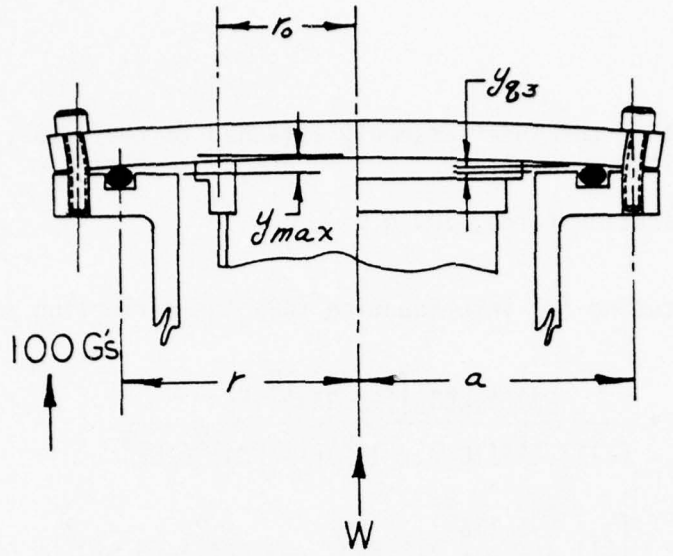

Figure 26 - Flanged joint,
cover distortion due to vertical
acceleration loading

Assuming the bolts are equally loaded, the tension in the bolts (F_{b3}) from (47) is

$$F_{b3} = \frac{W}{n} = \frac{4,050}{24} = 169 \text{ lbs}$$

5.5.4 Loading Condition 4 - Central Couple

Determine the deflection (y_{q4}) in the cover of the O-ring and tension in the bolts (F_{b4}) for an acceleration load of 100gs acting laterally on the inner assembly which is attached to the cover (Fig.27).

Assuming a fixed edge condition for the support of the cover, as before and using Case 10, Ref. 8, the angular deflection (θ_{max}) of the cover (at the center) is given by the formula

$$\theta_{max} = \frac{M}{\alpha E t^3} \qquad (50)$$

where M = 33,900 in.-lbs is the approximate moment that is acting on the cover and results from the product of the static moment (M_1=339) from Fig. 21C of this report and the 100g acceleration load factor. The factor α represents a variable coefficient and depends upon the ratio r_o/a which is

$$\frac{r_o}{a} = \frac{5.156}{5.843} = 0.882$$

For the ratio of 0.882 the value of α is 314 minimum, which was taken from the tables in Ref. 8, page 216. The other factors E and t are Young's modulus and the cover thickness respectively, and have the same values as in the previous calculations

Substituting the appropriate values into Equation (50) gives

$$\theta_{max} = \frac{33,900}{(314)(10.3 \times 10^6)(.5)^3} = 8.4 \times 10^{-5} \text{ radians}$$

Converting to degrees, minutes and seconds

$$\theta_{max} = (8.4 \times 10^{-5})(\frac{180}{\pi}) = 0.0048^o$$

$$\theta_{max} = 0^o\ 0'\ 17''$$

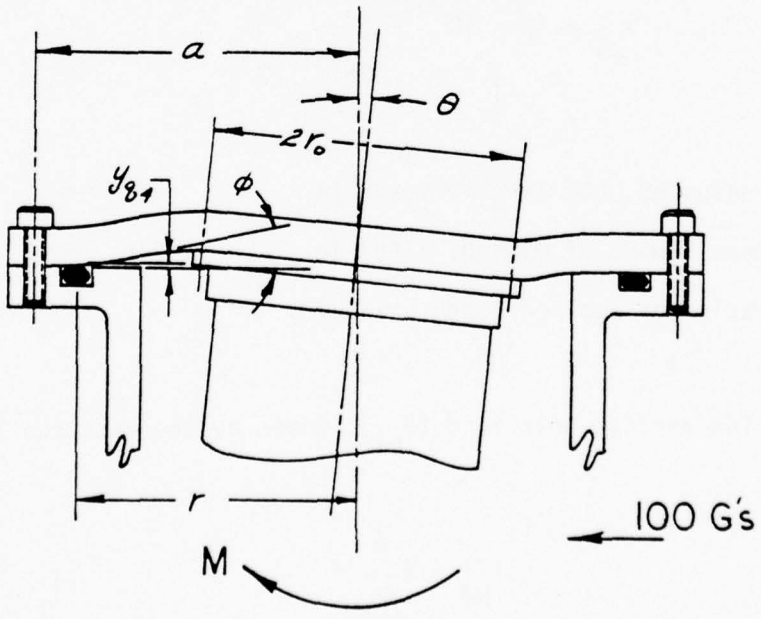

Figure 27 - Flanged Joint,
cover distortion due to trunnion loading

By triangulation the angle ϕ is given by the formula

$$\sin^{-1}\phi = \frac{r_o \sin\theta_{max}}{(a-r_o)} \tag{51}$$

from which

$$\sin^{-1}\phi = \frac{5.156 \sin 0.0048}{(5.843-5.156)} = .036^o$$

The deflection in the cover at the O-ring (y_{q4}) is then given by

$$y_{q4} = (a-r)\tan\phi \tag{52}$$

from which

$$y_{q4} = (5.843-5.587)\tan 0.036^o$$

$$y_{q4} = 16 \times 10^{-5} \text{ in.}$$

where

a = radius of bolt circle, 5.843 in.

r = mean radius of O-ring, 5.587 in.

r_o = radius of applied load, 5.156 in.

The applied bolt load (F_{b4}), given by the equation in Ref. 9, is

$$F_{b4} = \left(\frac{M}{\pi a}\right) f \tag{53}$$

where

f = bolt factor, (Fig.2, Ref.9)

1) for 8 bolts, f = .75

2) for 12 bolts, f = .51

3) for 18 bolts, f = .32

4) for 24 bolts, f = .25

Substituting values into Equation (53) gives

$$F_{b4} = \left(\frac{33,900}{5.843\pi}\right)(.25) = 462 \text{ lbs}$$

By superposition the total deflection (y_q) of the cover at the O-ring and the total applied load to the cover bolts are given by the following expressions

$$y_q = \sum y_{qn} = y_{q1} + y_{q2} + y_{q3} + y_{q4} \tag{54}$$

from which

$$y_q = (1.8 + 0.065 + 1.7 + 16)10^{-5}$$

$$y_q = 0.0002 \text{ in.}$$

and the total applied bolt load is

$$F_b = \sum F_{bn} = F_{b1} + F_{b2} + F_{b3} + F_{b4} \tag{55}$$

from which

$$F_b = (38.5 + 22 + 169 + 462)$$

$$F_b = 692 \text{ lbs}$$

From this analysis, the total displacement of the cover at the seal and the maximum force imposed on the bolts was found to be 0.0002 in. and 692 lbs respectively.

5.5.5 Resultant Bolt Tension and Compression of Members

24 #10-32 UNF x 5/8 in. long unbrako 1960 series socket heat cap screws was selected for clamping the members. The material of the screws is a high grade cadmium-plated alloy steel. The mechanical properties and application data that follow were obtained from Ref. 10, page 9

tensile strength (S_u) = 190,000 psi min

yield strength (S_y) = 170,000 psi min

seating torque (T) = 57 in.-lbs; based on an induced tensile stress of 100,000 psi

The pre-load (F_i) induced in the bolts after torquing to manufacturer's specifications is

$$F_i = SA_t = (100,000)(.02) = 2,000 \text{ lbs} \tag{56}$$

where

s = induced tensile stress in screw threads, 100,000 psi

A_t = tensile area of screw thread, .02 in.^{2}

The resultant tension (F_t) on the bolts is given by the expression

$$F_t = \frac{K_b F_b}{K_b + K_c} + F_i \tag{57}$$

where

K_b = spring constant of the bolt, 9.28×10^5 lbs/in.

K_c = spring constant of clamped members, 2.48×10^6 lbs/in.

F_b = applied bolt load, 692 lbs

F_i = bolt preload, 2,000 lbs

Rearranging Equation (45) and substituting in the appropriate values, the estimated spring constant of the bolts (K_b) is

$$K_b = \frac{AE}{L} = \frac{(.02)(29 \times 10^6)}{.625} = 9.28 \times 10^5 \text{ lbs/in.} \qquad (58)$$

The spring constant (K_c) of the clamped members is given by the pressure cone shown in Figure 28b and represents the material under the bolt head which resists the bolt load (Ref. 11). Assuming a pressure cone half angle of 15^0, the amount of load required to deflect the pressure cone one inch (K_b) is

$$K_c = \frac{\pi Ed \tan\phi}{\ln\left[\frac{D(2h\tan\phi+D)+d(2h\tan\phi-d)}{D(2h\tan\phi+D)-d(2h\tan\phi+d)}\right]} \qquad (59)$$

$$K_c = \frac{(3.14)(10.3 \times 10^6)(.196).268)}{\ln\left[\frac{.312(.167+.312)+.196(.167-.196)}{.312(.167+.312)-.196(.167+.196)}\right]}$$

$$K_c = 2.48 \times 10^6 \text{ lbs/in.}$$

where

D = seat diameter, .312 in.

d = hole diameter, .196 in.

h = flange thickness, .312 in.

ϕ = pressure cone angle, 15 degrees

E = Young's modulus for aluminum, 10.3×10^6

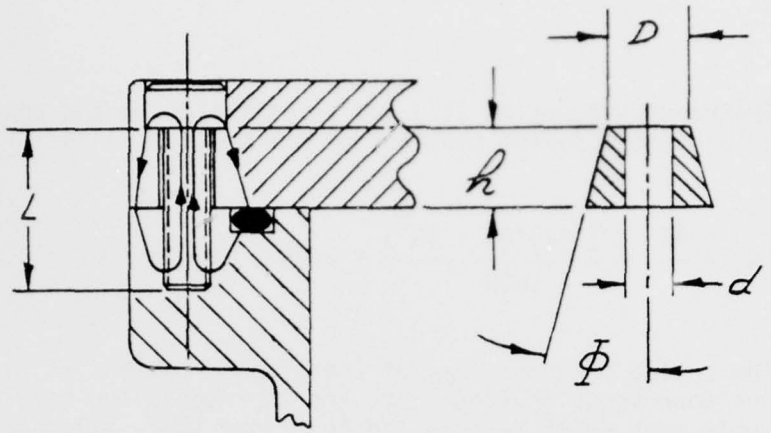

Figure 28a - Flanged Joint, bolt pressure distribution

Figure 28b - assumed pressure cone for members

Substituting the appropriate values in Equation (57), the resultant bolt tension is

$$F_t = \frac{(9.28 \times 10^5)(692)}{(.928 + 2.48)10^6} = 2,000$$

$$F_t = 2,188 \text{ lbs} \quad \underline{\textit{tension}}$$

In the same manner, the resultant compression (F_c) on the members is given by

$$F_c = \frac{K_c F_b}{K_c + K_b} - F_i \qquad (60)$$

from which

$$F_c = \frac{(2.48 \times 10^6)(692)}{(.928 + 2.48)10^6} - 2,000$$

and

$$F_c = -1,496 \text{ lbs} \quad \underline{\text{compression}}$$

The fact that (F_c) is negative would indicate that the bolt pre-load does indeed maintain a compressive load on the connected members.

The tensile strength of the clamping screws (F_u) from Equation (56) gives

$$F_u = S_u A_t = 190{,}000 \times .02$$

$$F_u = 3{,}800 \text{ lbs}$$

The resultant tensile load on the bolts from (57) was found to be 2,188 lbs. The factor of safety against failure of the bolts is given by

$$F.S. = \frac{F_u}{F_t} = \frac{3800}{2188} = 1.74$$

5.6 Telescope Structure - Joint Design

This section presents the design of the coupling joint for the telescope structure and focuses on the flange thickness, clamping pressure and thermal resistance across the interface.

5.6.1 Flange

In the design of the flanged coupling joints, it is a general rule to proportion the flange thickness approximately 1.5 to 1.75 times the clamping screw's diameter. In this application, where good thermal conduction across the interface is required, the general rule theory was deviated from to enhance the rigidity of the flange and the flange thickness was made 2.5 times the screw's body diameter. From this, the thickness (t) of the flange is estimated to be

$$t = 2.5(d) = (2.5)(.190) = .475 \text{ in.} \qquad (61)$$

where

d = body diameter of #10-24 unc screw, .190 in. dia.

A thickness of 1/2 in. was selected for the flange.

5.6.2 Clamping Pressure

Twenty-four (24) #10-24 unc, 7/8 in. long unbrako cap screws are used for clamping the joint. From Ref. 10, page 14, for type 304 stainless steel screws, the mechanical properties are

tensile strength, S_u = 80,000 psi

yield strength, S_y = 40,000 psi

seating torque, T = 40 in.-lbs

tensile strength, F_u = 1,360 lbs.

From figure 22c, page 45, the applied static moment of the joint at the interface was determined to be 195 in.-lbs. For a 100 g loading and using Equation (49), the moment imposed on the joint is

$$M = (195)(100) = 19{,}500 \text{ in.-lbs}$$

The maximum load on a single screw (F_b) can be calculated by using Equation (53) from which

$$F_b = \left[\frac{19{,}500}{(3.14)(4.25)} \right] 0.25 = 365 \text{ lbs.}$$

The pre-load (F_i) induced in the screws after torquing to manufacturing specifications is given by Equation (56) from which

$$F_i = (60{,}000)(.017) = 1{,}020 \text{ lbs}$$

where the maximum pre-load stress (S), based on 75 percent of the tensile strength (S_u), is 60,000 psi and the tensile area (A_t) is 0.017 in^2.

The spring constant of the screws is given by Equation (58) from which

$$K_b = \frac{(.017)(29 \times 10^6)}{.875} = 0.56 \times 10^6 \text{ lbs/in.}$$

The spring constant of the clamped members for an assumed pressure angle of 10^{0} is given by Equation (59) from which

$$K_c = \frac{(3.14)(10.3 \times 10^6)(.196)(.176)}{\ln\left[\frac{.312(.176+.312)+.196(.176-.196)}{.312(.176+.312)-.196(.176+.196)}\right]}$$

$$K_c = 1.78 \times 10^6 \text{ lbs/in.}$$

The resultant tension on a single screw is given by Equation (57) from which

$$F_t = \frac{(.56)(365)10^6}{(.56+1.78)10^6} = 1.020 = 1,107 \text{ lbs}$$

The factor of safety of the screws against failure is

$$F.S. = \frac{1360}{1107} = 1.23$$

The compression on the clamped members per screw is given by Equation (60) from which

$$F_c = \frac{(1.78)(365)10^6}{(.56+1.78)10^6} - 1020 = -742 \text{ lbs}$$

Assuming uniform compression loading per screw on the clamped members, the estimated clamping pressure (P) for the estimated area is

$$P = \frac{F_c n}{A_c} = \frac{(-742)(24)}{19.44} = 916 \text{ psi} \qquad (62)$$

where

F_c = compression/screw, ~742 lbs

A_c = contact area, 10.44 $in.^2$

n = number of screws, 24

5.6.3 Contact Resistance

The thermal resistance across the joint interface depends upon the surface finish, flatness, temperature and clamping pressure. Thermal resistance of interfaces at room temperature as a function of clamping pressure is given using Curve 2, figure 8, page 3-15 of Ref. 12. Two aluminum surfaces machined to a 10 RMS finish and clamped together with a pressure across the surface of 916 psi and housed in a vacuum environment is estimated to have a resistance per unit area of .1365^oK-in^2/watt. For a surface area of 19.44 in^2, the estimated contact resistance of the joint at a mean temperature of 316^oK is

$$R = \left(\frac{.1365^oK\text{-}in^2}{watt}\right)\left(\frac{1}{19.44\ in^2}\right) = 7.02 \times 10^{-3}{}^oK/watt$$

which simply indicates that a temperature difference of $7.02 \times 10^{-3}{}^oK$ is required to conduct one watt of power across the interface at the mean temperature.

Contact resistance increases as temperature decreases. Assuming the contact resistance varies inversely to the temperature, it follows that

$$R_{6^oK} = \left(\frac{T_1}{T_2}\right) R \qquad (63)$$

from which

$$R_{6^oK} = \frac{(316)(7.02 \times 10^{-3})}{6} = 0.37\ K^o/watt$$

From this, the estimated temperature difference for one (1) milliwatt of power to flow across the interface is

$$\Delta T = QR$$

$$\Delta T = \left(\frac{1}{1000}\right)(.37) = 3.7 \times 10^{-4} {}^{o}K \qquad (64)$$

5.7 Forward Radiation Shield - Joint Design

This section like the previous, presents a typical joint design and focuses on the same objectives.

5.7.1 Flange

Unlike the relationship used in paragraph 5.6.1, the thickness of the flange was determined by using the general rule theory and proportioned 1.5 times the screw diameter, in order that the flange to skin thickness ratio be kept to about 4. From this, the thickness (t) of the flange is estimated to be

$$t = 1.5(d) = 1.5(.164) = .246 \text{ in.} \qquad (65)$$

where

d = body diameter of #8-32 unc screw, .164 in. dia.

5.7.2 Clamping pressure

Twelve (12) #8-32 unc, 1/2 in. long unbrako screws are used for clamping the joint. From Ref. 10, page 14, for type 304 stainless steel screws, the mechanical properties are

tensile strength, S_u = 80,000 psi

yield strength, S_y = 40,000 psi

seating torque, T = 29 in.-lbs

tensile strength, F_u = 1120 lbs

From Figure 21c page 41 the applied static moment of the joint at the interface was determined to be 51 in.-lbs. For 100g loading and using Equation (49) the moment imposed on the joint is

$$M = (51)(100) = 5,100 \text{ in.-lbs}$$

The maximum load on a single screw is

$$F_b = \left[\frac{5{,}100}{(3.14)(4.937)} \right] .51 = 168 \text{ lbs}$$

where the bolt circle radius is 4.937 in. and the bolt factor, f is 0.51 which is based on a 12 hole equally spaced bolt pattern. Refer to paragraph 5.5.4, Equation (53).

The screw pre-load due to tightening is

$$F_i = (60{,}000)(.014) = 840\#$$

The spring constant of the screw is

$$K_b = \frac{(.014)(29 \times 10^6)}{5} = .812 \times 10^6 \text{ lbs/in.}$$

The spring constant of the clamped members for an assumed pressure angle of 30^0 is

$$K_c = \frac{3.2 \times 10^6}{\ln \left[\frac{.1508+.02}{.1508-.08} \right]} = 3.7 \text{ lbs/in.}$$

where the seat diameter, D is .270 in. and the hole diameter, d is .173 in.

The resultant tension on a single screw is

$$F_t = \frac{(.81)(168)10^6}{(.81+3.7)10^6} + 840 = 870 \text{ lbs}$$

The factor of safety of the screws against failure is

$$F.S. = \frac{1120}{870} = 1.29$$

The compression on the clamped members per screw is

$$F_c = \frac{(3.7)(168)10^6}{(.81+3.7)10^6} - 840 = -702 \text{ lbs}$$

Making the same assumptions as in paragraph 5.6.2 and using Equation (62) the pressure (P) in the interface is

$$P = \frac{(702)(12)}{16.52} = 510 \text{ psi}$$

where the contact area (A_c) was determined to be 16.52 in.^{2}

5.7.3 Contact Resistance

From Ref. 12, page 3-15, using curve 2 in figure 8, the thermal resistance of two aluminum surfaces machined to a 32 RMS finish, clamped together with a pressure of 510 psi and housed in a vacuum environment is estimated to be 0.556^{o}K-in^2/watt. For a surface area of 16.52 in.^{2}, the estimated contact resistance of the joint at a mean temperature of 316^{o}K is

$$R = \left(\frac{.556^oK\text{-in}^2}{\text{watt}}\right)\left(\frac{1}{16.52 \text{ in}^2}\right)$$

$$R = 3.4 \times 10^{-2} {}^oK/\text{watt}$$

The temperature in the interface of the radiation shield and support ring is predicted to be 70^{o}K. From Equation (63) the contact resistance in the interface is

$$R_{70^oK} = \frac{(316)(3.4 \times 10^{-2})}{70} = 0.153^oK/\text{watt}$$

As in paragraph 5.6.3, Equation (64), the estimated temperature difference for one (1) milliwatt of power to flow across the interface is

$$\Delta T = \left(\frac{1}{1000}\right)(.153) = 1.53 \times 10^{-4} {}^oK$$

5.8 Insulating Trunnion Support

The estimated heat leak of the insulating support discussed in paragraph 3.7 is determined here, which concludes the presentation of the mechanical design material. The calculations that follow are based on the assumption that the cool-down temperature of the radiation shield will stabilize at $140^{o}R$ ($77^{o}K$).

5.8.1 *Thermal Contraction of the Support*

The wire cable of the insulating support assembly shown in figure 29, bridging the outer vessel to the forward radiation shield, is 1/16 in. dia. by 1.91 in. long and made of 304 stainless steel stranded wire (7 by 7). The wire cable undergoes a change in length (ΔL) during cool-down in a direction which tends to shorten the cable's length. The change in length requires a rather complex analysis because of a thermal gradient condition existing in the support.

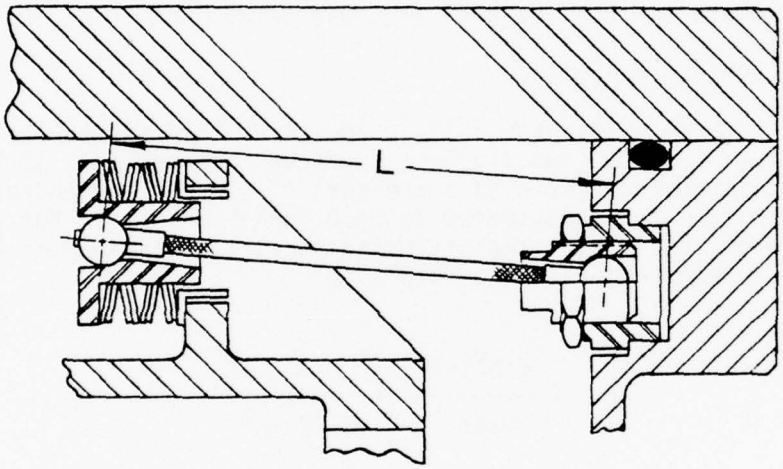

Figure 29 - Insulating Support

The unit thermal contraction ($\Delta L/L$) of the wire cable for a thermal gradient condition, while one end of the cable is cooled to $140^{o}R(77^{o}K)$ and the other end is maintained at $540^{o}R$ ($300^{o}K$) is given by the expression

$$\frac{\Delta L}{L} = \frac{\int_{T_c}^{T_h} e_t(T) K_t \, dT}{K_t (T_h - T_c)} \qquad \text{(Ref.4, page 467)} \qquad (66)$$

The integration of Equation (66) is carried out numerically. By using the trapezoidal rule for numerical integration and the property values for 304 stainless steel from Tables 7-6 and 7-7 (Ref.4, page 470), Table 3 is constructed.

$T(^oR)$	e_t 10^{-5}	$e_t(T)$ 10^{-3}	K_T Btu/hr-ft-^oF	$K_T e_t(T)$ 10^{-3}	$K_T e_t(T)\Delta T$ Btu/hr-ft
540	304	0	8.96	0	0
500	269	35	8.67	3.03	.0606
450	225	79	8.28	6.54	.2392
400	183	121	7.85	9.50	.4010
350	144	160	7.41	11.84	.5340
300	106	198	6.93	13.72	.6395
250	72	232	6.43	14.92	.7160
200	41	263	5.85	15.38	.7575
150	17	287	4.93	14.15	.7382
140	13	291	4.70	13.68	.1392

Table 3 -- Thermal Conductivity Integrals

Summing the values in the final column of Table 3, the value of the integral in the numerator of Equation (66) is

$$\int_{140^oR}^{540^oR} e_t(T)K_T dT = 4.186 \text{ Btu/hr-ft} \qquad (67)$$

From Appendix A-2, the mean thermal conductivity ($\bar{k}_T$) for 304 stainless steel between 140^{o}R and 540^{o}R is 7.206 Btu/hr-ft^2-^{o}R.

The thermal conductivity integral, the product of the mean conductivity and temperature range difference is given by

$$\int_{140^{o}R}^{540^{o}R} k_T dT = \bar{k}_T (T_h - T_c) \qquad (68)$$

from which

$$\int_{140^{o}}^{540^{o}} k_T dT = 7.206(540-140) = 2,882$$

Substituting the values found using Equations (67) and (68) in Equation (66), the unit thermal contraction for the cable is

$$\frac{\Delta L}{L} = \frac{4.225}{2,882} = 0.0015 \text{ in./in.}$$

Rearranging the terms in Equation (66), the total thermal contraction (ΔL) of the cable is

$$\Delta L = (1.91)(.0015) = 0.003 \text{ in.}$$

5.8.2 Wire Rope Tension

Several Belleville spring washers are used in the insulating support to allow the wire rope to contract freely during cool-down. The contraction of the wire rope is absorbed by the compression of the spring washers and in turn, induces a tensile force in it. In the previous paragraph, it was estimated that the wire rope would contract 0.003 inches. The computations for estimating the tension (T) in the wire rope for a nest of eight (8) Belleville spring washers stacked two (2) in parallel and (4) in series and compressed 0.003 in., is presented as follows.

From the stock list for part B0625-022 (Ref.2), the approximate cone height is 0.042 in. and the calculated load (P) at flat position is 105 lbs.

In a series arrangement the total deflection (δ_t) is given by the formula

$$\delta_t = (n_s)(\delta) \tag{69}$$

where (n_s) is the the number of washers in series and (δ) the deflection of a single washer. Substituting the contraction of the wire rope for the total deflection in Equation (69) and the number of series washers, then rearranging terms in the equation, the deflection of a single spring washer or a stack of parallel washers is

$$\delta = \frac{\delta_t}{n_s} = \frac{.003}{4} = 0.00075 \text{ in.} \tag{70}$$

The amount of dish (h) in the spring washer is

$$h = H - t = .042 - .022 = .02 \text{ in.} \tag{71}$$

where

H = cone height, .042 in.

t = stock thickness, .022 in.

The percent deflection (D) is

$$D = \frac{\delta}{h}(100) = \frac{.00075}{.02} \times 100 = 3.75\% \tag{72}$$

Using the h = t curve in figure 2 of Ref. 2 because the ratio

$$\frac{h}{t} = \frac{.020}{.022} \approx 1 \tag{73}$$

The estimated load at 3.75% deflection is approximately 5% of the load at flat position. The tension (T) in the wire rope is then found by the formula

$$T = .05(n_s)(n_p)(P) \tag{74}$$

from which

$$T = .05(4)(2)(105) = 42 \text{ lbs.}$$

where

n_s = number of washers in series, 4

n_p = number of washers in parallel, 2

P = load at flat position, 105 lbs.

5.8.3 Heat Leak

The following is a presentation of the method that was used in estimating the heat leak (Q) through the insulating supports for a temperature range of 300^{o} K to 77^{o} K. The heat leak is a function of the conductances of the Belleville washers and wire rope, designated by U_1 and U_2 respectively and the temperature difference across them. Formulated the heat flow equation is

$$Q = (U_1 + U_2)(\Delta T) \qquad (75)$$

A thermal model of the insulating support is shown in figure 30. The Belleville washers are illustrated by a series of parallel lines and the wire rope by a slender rod.

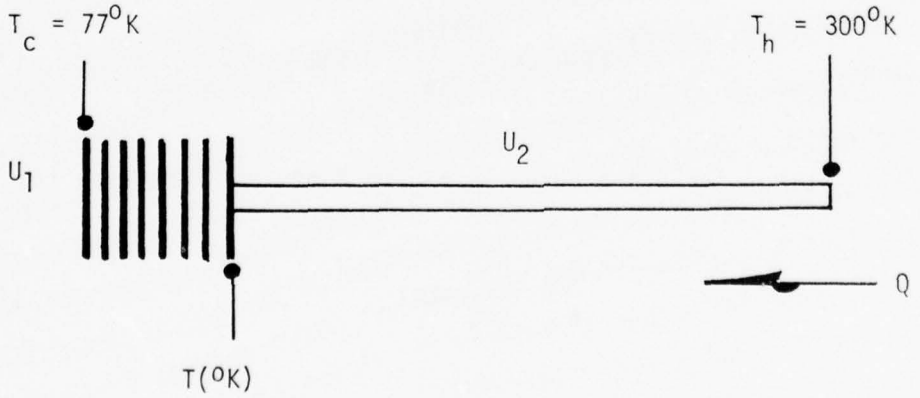

Figure 30 - Insulating Support Model

The electrical diagram shown in figure 31 is equivalent to the thermal model in which the Belleville washers and wire rope are now represented by their thermal resistances, R_1 and R_2.

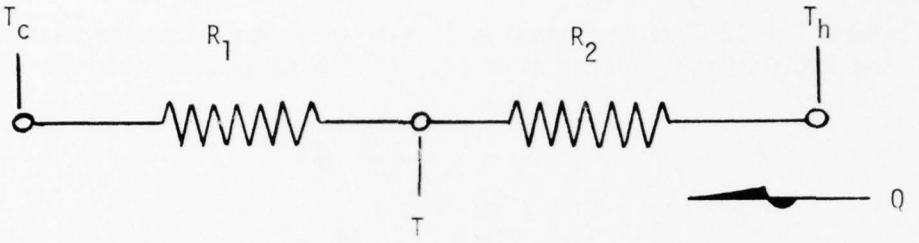

Figure 31 - Equivalent electrical series diagram

The thermal resistances shown in the series circuit diagram are given by the reciprocal of their conductances

$$R = \frac{1}{U_1} + \frac{1}{U_2} = R_1 + R_2 \qquad (76)$$

Rearranging the equation for U_1 and U_2 in terms of R_1 and R_2 and substituting in Equation (75), the heat flow equation in terms of thermal resistance is

$$Q = \frac{\Delta T}{R_1 + R_2} \qquad (77)$$

Using reference 13, Curve E of figure 4, the heat current conducted through forty-nine (49) .0195 in. thick round plates per square inch of contact area for a temperature interval of 296° K to 76° K is given by

$$W/in.^2 = 5 \left(\frac{p^{.67}}{750^{.67}}\right) \qquad (78)$$

where

p = Contact pressure, psi

The contact pressure (p) between plates is given by the expression

$$p = \frac{T}{A_c} \tag{79}$$

where T = 42 lbs, the tension in the wire rope estimated in 5.8.2 and the approximate contact area (A_c) of the plates is given by

$$A_c = \frac{\pi(D^2-d^2)}{4} \tag{80}$$

from which

$$A_c = \frac{3.14(.625^2-.317^2)}{4} = .228 \text{ in.}^2$$

where

D = outside diameter of washer, .625 in.
d = inside diameter of washer, .317 in.

Substituting the contact area and tension in Equation (79), the approximate contact pressure between washers is

$$p = \frac{42}{.228} \approx 200 \text{ psi}$$

and substituting the pressure (p) in Equation (78)

$$W/\text{in.}^2 = 5\left(\frac{200^{.67}}{750^{.67}}\right) = 2.06 \text{ W/in.}^2$$

Now, the heat conducted through eight (8) Belleville washers between the temperature of 296° K and 76° K is

$$Q_8 = \frac{W/\text{in.}^2 (A_c)(49)}{n} \tag{81}$$

from which

$$Q_8 = \frac{(2.06)(.228)(49)}{8} = 2.88 \text{ watts}$$

where

n = number of Belleville washers, 8

Rearranging the terms in Equation (77) and then substituting in the appropriate values, the thermal resistance (R_8) of eight parallel Belleville washers, between $300^{o}K$ - $77^{o}K$ is

$$R_8 = \frac{\Delta T}{Q_8} = \frac{(300-77)}{2.88} = 77.4^{o}K/\text{watt} \qquad (82)$$

It is assumed that the intermediate temperature (T) at the junction of the washers and wire rope is $82^{o}K$. The heat conduction ratio Q_1/Q_2 for solid members of the same material and dimensions between two temperature intervals ($300^{o}K$-$82^{o}K$ and $82^{o}K$-$77^{o}K$) is given by

$$Q_1/Q_2 = \frac{K_1(T_h-T)}{K_2(T-T_c)} \qquad (83)$$

from which

$$Q_1/Q_2 = \frac{.319(300-82)}{.210(82-77)} = 66$$

Therefore, the heat conduction (Q_2) at the lower temperature interval ($82^{o}K$-$77^{o}K$) is expressed by

$$Q_2 = \frac{Q_1}{66} \qquad (84)$$

Repeating the calculations, the conduction (Q_2) in terms of (Q_1) for several lower temperature ranges is expressed as follows

$$300^{o}K\text{-}87^{o}K \;\&\; 87^{o}K\text{-}77^{o}K,\; Q_2 = \frac{Q_1}{32} \tag{85}$$

$$300^{o}K\text{-}92^{o}K \;\&\; 92^{o}K\text{-}77^{o}K,\; Q_2 = \frac{Q_1}{21} \tag{86}$$

$$300^{o}K\text{-}97^{o}K \;\&\; 97^{o}K\text{-}77^{o}K,\; Q_2 = \frac{Q_1}{15} \tag{87}$$

where

K_1 & K_2 = mean thermal conductivity of 304 stainless steel. Their values are taken from the tables in Appendix A-2.

Now, assuming that the conduction ratios of the Belleville washers and solid member are the same, then, from Equations (84) through (87) the heat (Q_2) conducted through the Belleville washers for several temperature intervals are

letting $Q_1 = Q_8 = 2.88$ watts

$82^{o}K\text{-}77^{o}K,\; Q_2 = .044$ watts

$87^{o}K\text{-}77^{o}K,\; Q_2 = .090$ watts

$92^{o}K\text{-}77^{o}K,\; Q_2 = .140$ watts

$97^{o}K\text{-}77^{o}K,\; Q_2 = .190$ watts

Q_2 average = .116 watts

Using Equation (82) and the appropriate values, the thermal resistance (R_1) of the Belleville washers for typical temperature intervals are as follows

$82^{o}K$-$77^{o}K$, $R_1 = 114^{o}K/watt$

$87^{o}K$-$77^{o}K$, $R_1 = 111^{o}K/watt$

$92^{o}K$-$77^{o}K$, $R_1 = 107^{o}K/watt$

$97^{o}K$-$77^{o}K$, $R_1 = 105^{o}K/watt$

The average resistance $R_1 = 109^{o}K/watt$

Rearranging the terms again in Equation (77) and substituting in the average values of heat flow (Q_2) and resistance R_1, the temperature drop (ΔT) across the Belleville washers is

$$\Delta T = (R_1)(Q_2) = (109)(.116) = 13^{o}K \tag{88}$$

and from

$$\Delta T = (T-77) \tag{89}$$

The intermediate temperature (T) is given by

$$T = (77 + \Delta T) \tag{90}$$

from which

$$T = (77 + 13) = 90^{o}K$$

The resistance (R_2) of the wire rope is given by the formula

$$R_2 = \frac{L}{K_2 A_2} \tag{91}$$

where

L = length of wire rope, 1.91 in.

K = thermal conductivity of 304 stainless steel from table A-2 between $300^{o}K$-$90^{o}K$, .322 $W/in.^2\text{-}^{o}K$

and the area (A_2) of the 7x7 wire cable is

$$A_2 = 49\left(\frac{\pi D^2}{4}\right) \tag{92}$$

from which

$$A_2 = 49\left[\frac{(3.14)(.007)^2}{4}\right] = .001886 \text{ in.}^2$$

where

D = diameter of a single wire, .007 in.

Substituting the appropriate values in Equation (91), the resistance (R_2) of the wire cable is

$$R_2 = \frac{1.91}{(.322)(.001886)} = 3{,}145 \ ^{o}K/\text{watt}$$

Using Equation (77), the estimated heat leak through the insulating supports is

$$Q = 4\left[\frac{(300-77)}{109+3{,}145}\right] = 0.274 \text{ watts}$$

APPENDIX A

MEAN THERMAL CONDUCTIVITY

Mean thermal conductivities of four (4) common materials used in the model sensor are presented on the following pages in tabulated form. These conductivities were computed from graphical data referred to on this page.

Description	Reference	Page
1. Mean Thermal Conductivity Aluminum (6061-T6)	14	3.232
2. Mean Thermal Conductivity Stainless Steel (304)	15	489
3. Mean Thermal Conductivity Fiberglass, through thickness (in a vacuum)	15	419
4. Mean Thermal Conductivity fiberglass, normal to thickness (in a vacuum)	15	419

MEAN THERMAL CONDUCTIVITY
OF
ALUMINUM (6061-T6)

TEMPERATURE RANGE DEGREES KELVIN (K)	MEAN THERMAL CONDUCTIVITY WATTS/CM-K	MEAN THERMAL CONDUCTIVITY WATTS/IN-K	TEMPERATURE RANGE DEGREES RANKIN (R)	MEAN THERMAL CONDUCTIVITY BTU/HR-FT-R
4.0 - 300.0	1.204	3.058	7.2 - 540.0	69.582
6.0 - 300.0	1.212	3.078	10.8 - 540.0	70.021
8.0 - 300.0	1.219	3.097	14.4 - 540.0	70.452
10.0 - 300.0	1.226	3.115	18.0 - 540.0	70.876
12.0 - 300.0	1.234	3.134	21.6 - 540.0	71.293
14.0 - 300.0	1.241	3.152	25.2 - 540.0	71.701
16.0 - 300.0	1.248	3.169	28.8 - 540.0	72.103
18.0 - 300.0	1.255	3.186	32.4 - 540.0	72.496
20.0 - 300.0	1.261	3.203	36.0 - 540.0	72.880
22.0 - 300.0	1.268	3.220	39.6 - 540.0	73.257
24.0 - 300.0	1.274	3.236	43.2 - 540.0	73.625
26.0 - 300.0	1.280	3.252	46.8 - 540.0	73.985
28.0 - 300.0	1.286	3.267	50.4 - 540.0	74.335
30.0 - 300.0	1.292	3.282	54.0 - 540.0	74.677
32.0 - 300.0	1.298	3.297	57.6 - 540.0	75.009
34.0 - 300.0	1.304	3.311	61.2 - 540.0	75.331
36.0 - 300.0	1.309	3.325	64.8 - 540.0	75.644
38.0 - 300.0	1.314	3.338	68.4 - 540.0	75.947
40.0 - 300.0	1.319	3.351	72.0 - 540.0	76.240
42.0 - 300.0	1.324	3.364	75.6 - 540.0	76.526
44.0 - 300.0	1.329	3.376	79.2 - 540.0	76.806
46.0 - 300.0	1.334	3.388	82.8 - 540.0	77.081
48.0 - 300.0	1.339	3.400	86.4 - 540.0	77.352
50.0 - 300.0	1.343	3.412	90.0 - 540.0	77.618
52.0 - 300.0	1.348	3.423	93.6 - 540.0	77.879

26.0 - 100.0	.841	2.136	46.8 - 180.0	48.595
28.0 - 100.0	.852	2.163	50.4 - 180.0	49.214
30.0 - 100.0	.862	2.189	54.0 - 180.0	49.813
4.0 - 90.0	.667	1.694	7.2 - 162.0	38.552
6.0 - 90.0	.681	1.729	10.8 - 162.0	39.348
8.0 - 90.0	.695	1.764	14.4 - 162.0	40.135
10.0 - 90.0	.708	1.798	18.0 - 162.0	40.914
12.0 - 90.0	.721	1.832	21.6 - 162.0	41.684
14.0 - 90.0	.734	1.866	25.2 - 162.0	42.443
16.0 - 90.0	.747	1.898	28.8 - 162.0	43.192
18.0 - 90.0	.760	1.931	32.4 - 162.0	43.928
20.0 - 90.0	.773	1.963	36.0 - 162.0	44.651
4.0 - 80.0	.623	1.581	7.2 - 144.0	35.976
6.0 - 80.0	.637	1.618	10.8 - 144.0	36.810
8.0 - 80.0	.651	1.654	14.4 - 144.0	37.636
10.0 - 80.0	.665	1.690	18.0 - 144.0	38.455
12.0 - 80.0	.679	1.726	21.6 - 144.0	39.266
14.0 - 80.0	.693	1.761	25.2 - 144.0	40.067
16.0 - 80.0	.707	1.796	28.8 - 144.0	40.858
18.0 - 80.0	.721	1.830	32.4 - 144.0	41.638
20.0 - 80.0	.734	1.864	36.0 - 144.0	42.405
4.0 - 70.0	.572	1.452	7.2 - 126.0	33.042
6.0 - 70.0	.587	1.491	10.8 - 126.0	33.914
8.0 - 70.0	.602	1.529	14.4 - 126.0	34.781
10.0 - 70.0	.617	1.567	18.0 - 126.0	35.641
12.0 - 70.0	.632	1.604	21.6 - 126.0	36.494
14.0 - 70.0	.646	1.641	25.2 - 126.0	37.339
16.0 - 70.0	.661	1.678	28.8 - 126.0	38.175
18.0 - 70.0	.675	1.714	32.4 - 126.0	39.002
20.0 - 70.0	.689	1.750	36.0 - 126.0	39.818

A-1 (cont.)

54.0 - 300.0	1.352	3.434	97.2 - 540.0	78.137
56.0 - 300.0	1.357	3.446	100.8 - 540.0	78.390
58.0 - 300.0	1.361	3.457	104.4 - 540.0	78.640
60.0 - 300.0	1.365	3.467	108.0 - 540.0	78.886
62.0 - 300.0	1.369	3.478	111.6 - 540.0	79.128
64.0 - 300.0	1.373	3.488	115.2 - 540.0	79.368
66.0 - 300.0	1.378	3.499	118.8 - 540.0	79.604
68.0 - 300.0	1.382	3.509	122.4 - 540.0	79.837
70.0 - 300.0	1.386	3.519	126.0 - 540.0	80.068
72.0 - 300.0	1.389	3.529	129.6 - 540.0	80.296
74.0 - 300.0	1.393	3.539	133.2 - 540.0	80.523
76.0 - 300.0	1.397	3.549	136.8 - 540.0	80.747
78.0 - 300.0	1.401	3.559	140.4 - 540.0	80.970
80.0 - 300.0	1.405	3.569	144.0 - 540.0	81.192
82.0 - 300.0	1.409	3.578	147.6 - 540.0	81.412
84.0 - 300.0	1.413	3.588	151.2 - 540.0	81.632
86.0 - 300.0	1.416	3.598	154.8 - 540.0	81.852
88.0 - 300.0	1.420	3.607	158.4 - 540.0	82.071
90.0 - 300.0	1.424	3.617	162.0 - 540.0	82.290
4.0 - 100.0	.707	1.795	7.2 - 180.0	40.840
6.0 - 100.0	.720	1.828	10.8 - 180.0	41.600
8.0 - 100.0	.733	1.861	14.4 - 180.0	42.351
10.0 - 100.0	.746	1.894	18.0 - 180.0	43.093
12.0 - 100.0	.758	1.926	21.6 - 180.0	43.824
14.0 - 100.0	.771	1.958	25.2 - 180.0	44.545
16.0 - 100.0	.783	1.989	28.8 - 180.0	45.254
18.0 - 100.0	.795	2.020	32.4 - 180.0	45.951
20.0 - 100.0	.807	2.050	36.0 - 180.0	46.635
22.0 - 100.0	.819	2.079	39.6 - 180.0	47.304
24.0 - 100.0	.830	2.108	43.2 - 180.0	47.958

A-1 (cont.)

MEAN THERMAL CONDUCTIVITY
OF
304 STAINLESS STEEL)

TEMPERATURE RANGE DEGREES KELVIN (K)	MEAN THERMAL CONDUCTIVITY WATTS/CM-K	MEAN THERMAL CONDUCTIVITY WATTS/IN-K	TEMPERATURE RANGE DEGREES RANKIN (R)	MEAN THERMAL CONDUCTIVITY BTU/HR-FT-R
4.0 - 300.0	.105	.267	7.2 - 540.0	6.069
6.0 - 300.0	.106	.269	10.8 - 540.0	6.109
8.0 - 300.0	.106	.270	14.4 - 540.0	6.148
10.0 - 300.0	.107	.272	18.0 - 540.0	6.187
12.0 - 300.0	.108	.274	21.6 - 540.0	6.226
14.0 - 300.0	.108	.275	25.2 - 540.0	6.264
16.0 - 300.0	.109	.277	28.8 - 540.0	6.301
18.0 - 300.0	.110	.279	32.4 - 540.0	6.338
20.0 - 300.0	.110	.280	36.0 - 540.0	6.375
22.0 - 300.0	.111	.282	39.6 - 540.0	6.411
24.0 - 300.0	.112	.283	43.2 - 540.0	6.446
26.0 - 300.0	.112	.285	46.8 - 540.0	6.481
28.0 - 300.0	.113	.286	50.4 - 540.0	6.515
30.0 - 300.0	.113	.288	54.0 - 540.0	6.549
32.0 - 300.0	.114	.289	57.6 - 540.0	6.582
34.0 - 300.0	.114	.291	61.2 - 540.0	6.614
36.0 - 300.0	.115	.292	64.8 - 540.0	6.646
38.0 - 300.0	.116	.294	68.4 - 540.0	6.678
40.0 - 300.0	.116	.295	72.0 - 540.0	6.708
42.0 - 300.0	.117	.296	75.6 - 540.0	6.738
44.0 - 300.0	.117	.297	79.2 - 540.0	6.768
46.0 - 300.0	.118	.299	82.8 - 540.0	6.797
48.0 - 300.0	.118	.300	86.4 - 540.0	6.826
50.0 - 300.0	.119	.301	90.0 - 540.0	6.854
52.0 - 300.0	.119	.302	93.6 - 540.0	6.882

54.0 - 300.0	.120	.304	97.2 - 540.0	6.909
56.0 - 300.0	.120	.305	100.8 - 540.0	6.936
58.0 - 300.0	.120	.306	104.4 - 540.0	6.963
60.0 - 300.0	.121	.307	108.0 - 540.0	6.989
62.0 - 300.0	.121	.308	111.6 - 540.0	7.014
64.0 - 300.0	.122	.309	115.2 - 540.0	7.040
66.0 - 300.0	.122	.311	118.8 - 540.0	7.065
68.0 - 300.0	.123	.312	122.4 - 540.0	7.089
70.0 - 300.0	.123	.313	126.0 - 540.0	7.113
72.0 - 300.0	.124	.314	129.6 - 540.0	7.137
74.0 - 300.0	.124	.315	133.2 - 540.0	7.160
76.0 - 300.0	.124	.316	136.8 - 540.0	7.183
78.0 - 300.0	.125	.317	140.4 - 540.0	7.206
80.0 - 300.0	.125	.318	144.0 - 540.0	7.228
82.0 - 300.0	.125	.319	147.6 - 540.0	7.250
84.0 - 300.0	.126	.320	151.2 - 540.0	7.272
86.0 - 300.0	.126	.321	154.8 - 540.0	7.293
88.0 - 300.0	.127	.321	158.4 - 540.0	7.314
90.0 - 300.0	.127	.322	162.0 - 540.0	7.335
4.0 - 100.0	.056	.142	7.2 - 180.0	3.227
6.0 - 100.0	.057	.145	10.8 - 180.0	3.291
8.0 - 100.0	.058	.147	14.4 - 180.0	3.355
10.0 - 100.0	.059	.150	18.0 - 180.0	3.418
12.0 - 100.0	.060	.153	21.6 - 180.0	3.481
14.0 - 100.0	.061	.156	25.2 - 180.0	3.544
16.0 - 100.0	.062	.158	28.8 - 180.0	3.606
18.0 - 100.0	.063	.161	32.4 - 180.0	3.667
20.0 - 100.0	.065	.164	36.0 - 180.0	3.728
22.0 - 100.0	.066	.167	39.6 - 180.0	3.788
24.0 - 100.0	.067	.169	43.2 - 180.0	3.848

A-2 (cont.)

26.0 - 100.0	.068	.172	46.8 - 180.0	3.906
28.0 - 100.0	.069	.174	50.4 - 180.0	3.964
30.0 - 100.0	.070	.177	54.0 - 180.0	4.022
4.0 - 90.0	.052	.131	7.2 - 162.0	2.979
6.0 - 90.0	.053	.134	10.8 - 162.0	3.045
8.0 - 90.0	.054	.137	14.4 - 162.0	3.110
10.0 - 90.0	.055	.140	18.0 - 162.0	3.175
12.0 - 90.0	.056	.142	21.6 - 162.0	3.240
14.0 - 90.0	.057	.145	25.2 - 162.0	3.305
16.0 - 90.0	.058	.148	28.8 - 162.0	3.369
18.0 - 90.0	.059	.151	32.4 - 162.0	3.432
20.0 - 90.0	.060	.154	36.0 - 162.0	3.495
4.0 - 80.0	.047	.119	7.2 - 144.0	2.713
6.0 - 80.0	.048	.122	10.8 - 144.0	2.781
8.0 - 80.0	.049	.125	14.4 - 144.0	2.848
10.0 - 80.0	.050	.128	18.0 - 144.0	2.916
12.0 - 80.0	.052	.131	21.6 - 144.0	2.982
14.0 - 80.0	.053	.134	25.2 - 144.0	3.049
16.0 - 80.0	.054	.137	28.8 - 144.0	3.115
18.0 - 80.0	.055	.140	32.4 - 144.0	3.180
20.0 - 80.0	.056	.143	36.0 - 144.0	3.245
4.0 - 70.0	.042	.107	7.2 - 126.0	2.430
6.0 - 70.0	.043	.110	10.8 - 126.0	2.500
8.0 - 70.0	.044	.113	14.4 - 126.0	2.569
10.0 - 70.0	.046	.116	18.0 - 126.0	2.638
12.0 - 70.0	.047	.119	21.6 - 126.0	2.706
14.0 - 70.0	.048	.122	25.2 - 126.0	2.775
16.0 - 70.0	.049	.125	28.8 - 126.0	2.843
18.0 - 70.0	.050	.128	32.4 - 126.0	2.910
20.0 - 70.0	.052	.131	36.0 - 126.0	2.977

A-2 (cont.)

MEAN THERMAL CONDUCTIVITY OF EPOXY FIBERGLASS LAMINATE THROUGH THICKNESS (IN A VACUUM)

TEMPERATURE RANGE DEGREES KELVIN (K)	MEAN THERMAL CONDUCTIVITY WATTS/CM-K	MEAN THERMAL CONDUCTIVITY WATTS/IN-K	TEMPERATURE RANGE DEGREES RANKIN (R)	MEAN THERMAL CONDUCTIVITY BTU/HR-FT-R
4.0 - 300.0	.002433	.006180	7.2 - 540.0	.1406
6.0 - 300.0	.002448	.006219	10.8 - 540.0	.1415
8.0 - 300.0	.002464	.006258	14.4 - 540.0	.1424
10.0 - 300.0	.002479	.006297	18.0 - 540.0	.1433
12.0 - 300.0	.002494	.006335	21.6 - 540.0	.1441
14.0 - 300.0	.002509	.006372	25.2 - 540.0	.1450
16.0 - 300.0	.002524	.006410	28.8 - 540.0	.1458
18.0 - 300.0	.002538	.006447	32.4 - 540.0	.1467
20.0 - 300.0	.002553	.006484	36.0 - 540.0	.1475
22.0 - 300.0	.002567	.006521	39.6 - 540.0	.1484
24.0 - 300.0	.002581	.006557	43.2 - 540.0	.1492
26.0 - 300.0	.002596	.006593	46.8 - 540.0	.1500
28.0 - 300.0	.002610	.006629	50.4 - 540.0	.1508
30.0 - 300.0	.002624	.006665	54.0 - 540.0	.1516
32.0 - 300.0	.002638	.006700	57.6 - 540.0	.1524
34.0 - 300.0	.002652	.006736	61.2 - 540.0	.1532
36.0 - 300.0	.002666	.006770	64.8 - 540.0	.1540
38.0 - 300.0	.002679	.006805	68.4 - 540.0	.1548
40.0 - 300.0	.002693	.006839	72.0 - 540.0	.1556
42.0 - 300.0	.002706	.006873	75.6 - 540.0	.1564
44.0 - 300.0	.002719	.006907	79.2 - 540.0	.1571
46.0 - 300.0	.002732	.006940	82.8 - 540.0	.1579
48.0 - 300.0	.002745	.006973	86.4 - 540.0	.1586
50.0 - 300.0	.002758	.007005	90.0 - 540.0	.1594

52.0 - 300.0	.002771	.007038	93.6 - 540.0	.1601
54.0 - 300.0	.002783	.007070	97.2 - 540.0	.1608
56.0 - 300.0	.002796	.007102	100.8 - 540.0	.1616
58.0 - 300.0	.002809	.007133	104.4 - 540.0	.1623
60.0 - 300.0	.002820	.007164	108.0 - 540.0	.1630
62.0 - 300.0	.002833	.007195	111.6 - 540.0	.1637
64.0 - 300.0	.002845	.007225	115.2 - 540.0	.1644
66.0 - 300.0	.002856	.007255	118.8 - 540.0	.1651
68.0 - 300.0	.002868	.007285	122.4 - 540.0	.1657
70.0 - 300.0	.002880	.007315	126.0 - 540.0	.1664
72.0 - 300.0	.002891	.007344	129.6 - 540.0	.1671
74.0 - 300.0	.002903	.007372	133.2 - 540.0	.1677
76.0 - 300.0	.002914	.007401	136.8 - 540.0	.1684
78.0 - 300.0	.002925	.007429	140.4 - 540.0	.1690
80.0 - 300.0	.002936	.007457	144.0 - 540.0	.1697
82.0 - 300.0	.002947	.007484	147.6 - 540.0	.1703
84.0 - 300.0	.002957	.007511	151.2 - 540.0	.1709
86.0 - 300.0	.002968	.007537	154.8 - 540.0	.1715
88.0 - 300.0	.002978	.007563	158.4 - 540.0	.1721
90.0 - 300.0	.002988	.007589	162.0 - 540.0	.1727
4.0 - 100.0	.001177	.002989	7.2 - 180.0	.0680
6.0 - 100.0	.001198	.003044	10.8 - 180.0	.0693
8.0 - 100.0	.001220	.003099	14.4 - 180.0	.0705
10.0 - 100.0	.001241	.003152	18.0 - 180.0	.0717
12.0 - 100.0	.001262	.003206	21.6 - 180.0	.0729
14.0 - 100.0	.001283	.003259	25.2 - 180.0	.0741
16.0 - 100.0	.001304	.003311	28.8 - 180.0	.0753
18.0 - 100.0	.001324	.003363	32.4 - 180.0	.0765
20.0 - 100.0	.001345	.003415	36.0 - 180.0	.0777
22.0 - 100.0	.001365	.003467	39.6 - 180.0	.0789

A-3 (cont.)

AD-A044 166 WENTWORTH INST BOSTON MASS F/G 17/5
MODEL SENSOR FOR PROJECT ZIP.(U)
MAR 77 J M OTIS F19628-76-C-0211
UNCLASSIFIED SCIENTIFIC-1 AFGL-TR-77-0088 NL

2 OF 2
ADA044166

END
DATE
FILMED
10-77
DDC

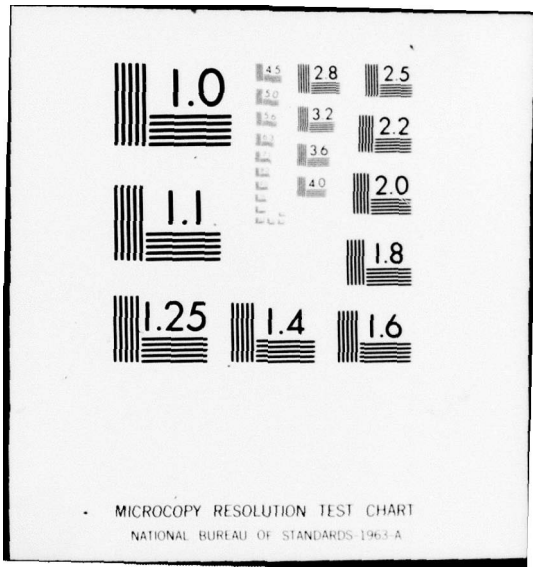
1.0
1.1
1.25
1.4
1.6
1.8
2.0
2.2
2.5
2.8
3.2
3.6
4.0
4.5
5.0
5.6
MICROCOPY RESOLUTION TEST CHART
NATIONAL BUREAU OF STANDARDS-1963-A

24.0 - 100.0	.001385	.003519	43.2 - 180.0	.0801
26.0 - 100.0	.001406	.003570	46.8 - 180.0	.0812
28.0 - 100.0	.001426	.003622	50.4 - 180.0	.0824
30.0 - 100.0	.001447	.003675	54.0 - 180.0	.0836
4.0 - 90.0	.001078	.002739	7.2 - 162.0	.0623
6.0 - 90.0	.001100	.002795	10.8 - 162.0	.0636
8.0 - 90.0	.001122	.002850	14.4 - 162.0	.0648
10.0 - 90.0	.001143	.002904	18.0 - 162.0	.0661
12.0 - 90.0	.001164	.002958	21.6 - 162.0	.0673
14.0 - 90.0	.001185	.003011	25.2 - 162.0	.0685
16.0 - 90.0	.001206	.003064	28.8 - 162.0	.0697
18.0 - 90.0	.001227	.003117	32.4 - 162.0	.0709
20.0 - 90.0	.001248	.003169	36.0 - 162.0	.0721
4.0 - 80.0	.000978	.002484	7.2 - 144.0	.0565
6.0 - 80.0	.001000	.002540	10.8 - 144.0	.0578
8.0 - 80.0	.001022	.002595	14.4 - 144.0	.0590
10.0 - 80.0	.001043	.002650	18.0 - 144.0	.0603
12.0 - 80.0	.001065	.002704	21.6 - 144.0	.0615
14.0 - 80.0	.001086	.002758	25.2 - 144.0	.0627
16.0 - 80.0	.001107	.002811	28.8 - 144.0	.0640
18.0 - 80.0	.001128	.002864	32.4 - 144.0	.0652
20.0 - 80.0	.001148	.002917	36.0 - 144.0	.0664
4.0 - 70.0	.000876	.002226	7.2 - 126.0	.0506
6.0 - 70.0	.000899	.002283	10.8 - 126.0	.0519
8.0 - 70.0	.000921	.002339	14.4 - 126.0	.0532
10.0 - 70.0	.000943	.002394	18.0 - 126.0	.0545
12.0 - 70.0	.000964	.002449	21.6 - 126.0	.0557
14.0 - 70.0	.000986	.002503	25.2 - 126.0	.0570
16.0 - 70.0	.001007	.002557	28.8 - 126.0	.0582
18.0 - 70.0	.001028	.002610	32.4 - 126.0	.0594
20.0 - 70.0	.001048	.002663	36.0 - 126.0	.0606

A-3 (cont.)

MEAN THERMAL CONDUCTIVITY
OF
EPOXY FIBERGLASS LAMINATE
NORMAL TO THICKNESS
(IN A VACUUM)

TEMPERATURE RANGE DEGREES KELVIN (K)	MEAN THERMAL CONDUCTIVITY WATTS/CM-K	MEAN THERMAL CONDUCTIVITY WATTS/IN-K	TEMPERATURE RANGE DEGREES RANKIN (R)	MEAN THERMAL CONDUCTIVITY BTU/HR-FT-R
4.0 - 300.0	.002301	.005845	7.2 - 540.0	.1330
6.0 - 300.0	.002312	.005873	10.8 - 540.0	.1336
8.0 - 300.0	.002323	.005901	14.4 - 540.0	.1343
10.0 - 300.0	.002334	.005929	18.0 - 540.0	.1349
12.0 - 300.0	.002345	.005956	21.6 - 540.0	.1355
14.0 - 300.0	.002355	.005982	25.2 - 540.0	.1361
16.0 - 300.0	.002366	.006008	28.8 - 540.0	.1367
18.0 - 300.0	.002376	.006034	32.4 - 540.0	.1373
20.0 - 300.0	.002386	.006060	36.0 - 540.0	.1379
22.0 - 300.0	.002396	.006086	39.6 - 540.0	.1385
24.0 - 300.0	.002406	.006111	43.2 - 540.0	.1390
26.0 - 300.0	.002416	.006137	46.8 - 540.0	.1396
28.0 - 300.0	.002426	.006162	50.4 - 540.0	.1402
30.0 - 300.0	.002436	.006188	54.0 - 540.0	.1408
32.0 - 300.0	.002446	.006213	57.6 - 540.0	.1414
34.0 - 300.0	.002456	.006239	61.2 - 540.0	.1419
36.0 - 300.0	.002467	.006265	64.8 - 540.0	.1425
38.0 - 300.0	.002477	.006291	68.4 - 540.0	.1431
40.0 - 300.0	.002487	.006317	72.0 - 540.0	.1437
42.0 - 300.0	.002497	.006343	75.6 - 540.0	.1443
44.0 - 300.0	.002508	.006370	79.2 - 540.0	.1449
46.0 - 300.0	.002518	.006396	82.8 - 540.0	.1455
48.0 - 300.0	.002529	.006423	86.4 - 540.0	.1461
50.0 - 300.0	.002539	.006449	90.0 - 540.0	.1467

52.0 - 300.0	.002550	.006476	93.6 - 540.0	.1473
54.0 - 300.0	.002560	.006503	97.2 - 540.0	.1480
56.0 - 300.0	.002571	.006530	100.8 - 540.0	.1486
58.0 - 300.0	.002582	.006558	104.4 - 540.0	.1492
60.0 - 300.0	.002593	.006585	108.0 - 540.0	.1498
62.0 - 300.0	.002604	.006613	111.6 - 540.0	.1505
64.0 - 300.0	.002615	.006641	115.2 - 540.0	.1511
66.0 - 300.0	.002626	.006669	118.8 - 540.0	.1517
68.0 - 300.0	.002637	.006697	122.4 - 540.0	.1524
70.0 - 300.0	.002648	.006726	126.0 - 540.0	.1530
72.0 - 300.0	.002659	.006755	129.6 - 540.0	.1537
74.0 - 300.0	.002671	.006784	133.2 - 540.0	.1543
76.0 - 300.0	.002682	.006813	136.8 - 540.0	.1550
78.0 - 300.0	.002694	.006843	140.4 - 540.0	.1557
80.0 - 300.0	.002706	.006873	144.0 - 540.0	.1564
82.0 - 300.0	.002718	.006903	147.6 - 540.0	.1571
84.0 - 300.0	.002730	.006934	151.2 - 540.0	.1578
86.0 - 300.0	.002742	.006965	154.8 - 540.0	.1585
88.0 - 300.0	.002754	.006996	158.4 - 540.0	.1592
90.0 - 300.0	.002767	.007028	162.0 - 540.0	.1599
4.0 - 100.0	.001195	.003034	7.2 - 180.0	.0690
6.0 - 100.0	.001206	.003064	10.8 - 180.0	.0697
8.0 - 100.0	.001217	.003091	14.4 - 180.0	.0703
10.0 - 100.0	.001227	.003117	18.0 - 180.0	.0709
12.0 - 100.0	.001237	.003142	21.6 - 180.0	.0715
14.0 - 100.0	.001246	.003165	25.2 - 180.0	.0720
16.0 - 100.0	.001254	.003186	28.8 - 180.0	.0725
18.0 - 100.0	.001262	.003206	32.4 - 180.0	.0730
20.0 - 100.0	.001270	.003226	36.0 - 180.0	.0734
22.0 - 100.0	.001277	.003244	39.6 - 180.0	.0738

A-4 (cont.)

24.0 - 100.0	.001284	.003262	43.2 - 180.0	.0742
26.0 - 100.0	.001291	.003279	46.8 - 180.0	.0746
28.0 - 100.0	.001298	.003296	50.4 - 180.0	.0750
30.0 - 100.0	.001304	.003313	54.0 - 180.0	.0754
4.0 - 90.0	.001163	.002955	7.2 - 162.0	.0672
6.0 - 90.0	.001176	.002986	10.8 - 162.0	.0679
8.0 - 90.0	.001187	.003015	14.4 - 162.0	.0686
10.0 - 90.0	.001194	.003043	18.0 - 162.0	.0692
12.0 - 90.0	.001208	.003068	21.6 - 162.0	.0698
14.0 - 90.0	.001217	.003092	25.2 - 162.0	.0704
16.0 - 90.0	.001226	.003115	28.8 - 162.0	.0709
18.0 - 90.0	.001235	.003136	32.4 - 162.0	.0713
20.0 - 90.0	.001242	.003156	36.0 - 162.0	.0718
4.0 - 80.0	.001129	.002868	7.2 - 144.0	.0653
6.0 - 80.0	.001142	.002901	10.8 - 144.0	.0660
8.0 - 80.0	.001154	.002932	14.4 - 144.0	.0667
10.0 - 80.0	.001166	.002961	18.0 - 144.0	.0674
12.0 - 80.0	.001176	.002988	21.6 - 144.0	.0680
14.0 - 80.0	.001186	.003013	25.2 - 144.0	.0686
16.0 - 80.0	.001196	.003037	28.8 - 144.0	.0691
18.0 - 80.0	.001204	.003059	32.4 - 144.0	.0696
20.0 - 80.0	.001212	.003080	36.0 - 144.0	.0701
4.0 - 70.0	.001092	.002774	7.2 - 126.0	.0631
6.0 - 70.0	.001106	.002809	10.8 - 126.0	.0639
8.0 - 70.0	.001119	.002842	14.4 - 126.0	.0647
10.0 - 70.0	.001131	.002873	18.0 - 126.0	.0654
12.0 - 70.0	.001142	.002901	21.6 - 126.0	.0660
14.0 - 70.0	.001153	.002928	25.2 - 126.0	.0666
16.0 - 70.0	.001162	.002952	28.8 - 126.0	.0672
18.0 - 70.0	.001171	.002976	32.4 - 126.0	.0677
20.0 - 70.0	.001180	.002997	36.0 - 126.0	.0682

A-4 (cont.)

REFERENCES

1. Tru-Loc Wire Rope Assemblies; American Chain and Cable Company, Inc. Wilkes-Barre, PA

2. Belleville Spring Washers; Associated Spring Corporation, Wallace Barnes Division, Bristol, Conn. 06012

3. Singer, F. L.; Engineering Mechanics, Second Edition, Harper and Brothers, publishers, N.Y. (1954)

4. Randall Barron; Cryogenic Systems, McGraw-Hill Book Company, N.Y.

5. Valance & Doughtie; Design of Machine Members, second edition McGraw-Hill Book Company, N.Y.

6. Parker Seal Co., Parker O-ring Handbook #OR5700, issued Jan. 1975, Lexington, Kentucky, 40509

7. Priest and Gilligan; Design Manual for High-strength Steels, third printing, 1956, U. S. Steel Corporation, Pittsburgh, PA

8. Roark; Formulas for Stress and Strain, third edition, 1954, McGraw-Hill Book Company, N.Y.

9. R. Bazaz; Maximum Bolt Tension in Flanged Connections, Machine Design September 29, 1966 edition

10. Standard Pressed Steel Co., Unbrako Socket Screws, Form 3625-50M-174-SPS, Jenkintown, Pennsylvania 19046

11. R. Little; Bolted Joints, Machine Design, November 9, 1967 edition, Penton Publishing Co., Cleveland, Ohio 44113

12. Hartnett, Handbook of Heat Transfer, McGraw-Hill

13. Mikesell and Scott; Heat Conduction Through Insulating Supports in Very Low Temperature Equipment, NBS Research paper #2726 Vol. 57, No. 6, Dec. '56

14. Johnson V., The Compendium of the Properties of Materials at Low Temperature (Phase I), Part II, Properties of Solids, WADD TECHNICAL REPORT 60-56, National Bureau of Standards, Cryogenic Engineering Laboratory, October 1960

15. F. H. Schwartzberg, Cryogenic Materials Data Handbook, Vol. II, AD-713-620, TDR-64-280, July 1970

☆ U.S. GOVERNMENT PRINTING OFFICE: 1977--700-002--115